1987

Incorporating the effect of exciter in the transient energy function method

Khashayar Nodehi
Iowa State University

INFORMATION TO USERS

While the most advanced technology has been used to photograph and reproduce this manuscript, the quality of the reproduction is heavily dependent upon the quality of the material submitted. For example:

- Manuscript pages may have indistinct print. In such cases, the best available copy has been filmed.
- Manuscripts may not always be complete. In such cases, a note will indicate that it is not possible to obtain missing pages.
- Copyrighted material may have been removed from the manuscript. In such cases, a note will indicate the deletion.

Oversize materials (e.g., maps, drawings, and charts) are photographed by sectioning the original, beginning at the upper left-hand corner and continuing from left to right in equal sections with small overlaps. Each oversize page is also filmed as one exposure and is available, for an additional charge, as a standard 35mm slide or as a 17"x 23" black and white photographic print.

Most photographs reproduce acceptably on positive microfilm or microfiche but lack the clarity on xerographic copies made from the microfilm. For an additional charge, 35mm slides of 6"x 9" black and white photographic prints are available for any photographs or illustrations that cannot be reproduced satisfactorily by xerography.

Nodehi, Khashayar

INCORPORATING THE EFFECT OF EXCITER IN THE TRANSIENT ENERGY FUNCTION METHOD

Iowa State University PH.D. 1987

Incorporating the effect of exciter in the transient energy function method

by

Khashayar Nodehi

A Dissertation Submitted to the

Graduate Faculty in Partial Fulfillment of the

Requirements for the Degree of

DOCTOR OF PHILOSOPHY

Department: Electrical Engineering and Computer Engineering
Major: Electrical Engineering (Electric Power)

Approved:

Signature was redacted for privacy.

In Charge of Major Work

Signature was redacted for privacy.

For the Major Department

Signature was redacted for privacy.

For the Graduate College

Iowa State University
Ames, Iowa

1987

TABLE OF CONTENTS

CHAPTER I. INTRODUCTION

Transient Stability

The dynamic behavior of a power system is governed by a mix of electrical, electromechanical, and thermomechanical variables. For a moderate size power system, these variables are related through a large number of differential equations and many algebraic equations; these equations are nonlinear. The dynamic response of a power system to disturbances involves transients which last from few micro-seconds to one hour.

Obviously, the degree of detail of representation and the simplifying assumptions that can be made are a function of the particular problem under study. For example, at the lower end of the time scale (micro-seconds) studies of switching transient voltages can be made neglecting entirely the generator electromechanical dynamics but representing the transmission lines in great detail. At the other end of the time scale, studies of tie-line power and frequency control and/or of the boiler response can be made neglecting entirely the transmission network and transients of the generators, but representing the boiler in detail. In between the two extremes are electromechanical transients of generators where the network transients as well as boiler response and load frequency control are neglected. Study of the generator electromechanical transients is the subject of power system stability studies. In such studies, the parameters which affect the electrical and mechanical torques are considered in detail. Among them are the

generator electrical parameters, inertia, and the excitation and turbine speed controls.

Stability studies are performed to determine whether following a disturbance, i) the generators remain in synchronism with respect to each other and the ensuing oscillations are damped, and ii) the system settles to an acceptable operating point, i.e., tie-line flows, voltage levels, etc., are within prespecified range. If condition (i) is satisfied, the system is said to be asymptotically stable.

The power system stability problem has traditionally been separated into categories of transient stability and steady-state stability. Roughly speaking, the steady state stability problem is the study of the power system response to small perturbations. Transient stability is concerned with the dynamic response of the system to large disturbances. Transient stability depends strongly on the magnitude and location of disturbance whereas dynamic stability tends to be a property of the state of the system [1, Chapter 1]. An important implication of such distinction between transient and steady-state stability is in the modeling requirements of each study. In a large interconnected system, the effect of a disturbance and tie-line oscillations can be felt in an area remote from the source of disturbance after several seconds.

Upon initiation of a major disturbance, e.g., a fault, the rotors of machines close to the fault location are subjected to large accelerating powers. As a result, these rotor angles start to increase. If

during the transient, some of the rotor angles increase indefinitely with respect to other generators in the system, these generators lose synchronism with the rest of the generators. The first swing of the generator rotor angles is of especial significance in transient stability studies. The authors of references [2 and 3] conclude that it is generally true that if first swing stability can be achieved, satisfactory performance of later swings can be assumed by proper design of controls. Therefore, transient stability is mainly a first swing phenomenon.

Traditionally, for first swing stability studies the "classical model" of the power system has been used. In the classical model, the generators are represented by a constant voltage behind transient reactance, their mechanical input powers are assumed constant, and the loads are modeled as constant impedances. The assumption of constant voltage behind transient reactance is equivalent to the assumption of constant flux linkage of the field winding.

A severe disturbance, e.g., a fault close to a generator, causes a substantial increase in the armature currents which results in a magnetomotive force in a direction which tends to oppose the flux linking the main field winding. Therefore, the excitation system during the faulted period acts in a manner to increase the flux linking the main field winding. The voltage regulator couples the output of synchronous machine (terminal voltage) to the input of the exciter through feedback and forward controlling elements for the purpose of regulating the

synchronous machine output [4]. Therefore, the response of the excitation system has an effect on transient behavior of the synchronous machines.

The subtlety of the classical model is that the effect of the exciter and voltage regulator are not entirely neglected although the machine is simply represented by a constant voltage behind transient reactance. If the transient is initiated by a fault, the effect of voltage regulator and armature reaction tend to counteract each other. These effects, along with the relatively long effective time constant of the main field winding [1], result in an almost constant flux linkage during the first swing. The effect of armature reaction is pronounced during the fault period [see Chapter 8 of reference 1]. Therefore, the duration of the fault and the time constants of excitation system are important factors in determining the validity of the classical model.

A study reported by Crary [5] illustrates that for faults of short duration the classical model corresponds to a very slow and weak excitation system. For longer fault durations (greater than 0.1 seconds), the classical model approaches excitation systems of response ratios of 2.0 p.u. or higher. Although these results correspond to a system of one machine connected to an infinite bus the general conclusions are true in the case of multi-machine power systems.

Effect of excitation systems on transient stability

Trends in design of power system components have resulted in lower stability margins. Economic and environmental considerations

combined with continual need to meet growing load demand have resulted in greater generator size and higher capacity transmission circuits. Economic operation and fuel conservation resulted in heavier loading of transmission and higher power transfer levels between adjacent systems. Modern generator units have lower inertia constant and higher reactances [6], both of which have adverse effects on stability. A number of control mechanisms have been suggested to improve stability. Reducing the accelerating power can be accomplished by reducing the mechanical power by fast valving, or by increasing the electrical power by fast acting excitation systems, or by inserting breaking resistor to help transient stability [2,3,6,7,8]. However, in the U.S.A., the excitation systems are often the primary control devices to combat the stability problem.

Valuable insight into the effect of the exciter-voltage regulator on stability has been obtained by studying the stability of synchronous machines under small perturbations. In stability studies, the phenomenon in question is the behavior of the rotor angle and speed following a disturbance. de Mello and Concordia [3] have studied the torque-speed-angle loop using frequency domain techniques. At any frequency of oscillation, torques are developed in phase with machine rotor angle (synchronizing torques) and torques in phase with machine rotor speed (damping torques). Stability can be endangered by lack of either or both synchronizing and damping torques. During disturbances, there is an urgent need for positive synchronizing torques to restore the rotor angles and prevent loss of synchronism. High gain voltage regulators provide syn-

chronizing torques. Therefore, fast acting high-gain exciter-voltage regulators are helpful in developing restoring forces during the first swing period. Although fast acting high-gain exciters aggravate the poor damping which already exists in a heavily loaded power system, sufficient damping can be provided by use of supplementary controls along with the excitation system.

Direct Methods of Transient Stability Analysis

Transient stability of power system is an increasingly important consideration in system planning and operation. Numerical integration of the differential equations representing the system transient behavior is the technique which is widely used for transient stability studies. In this method, the system equations are formulated in state-space form and time solution of all the state variables is obtained. One major drawback of the time solution technique is that it is computationally slow.

Speed of solution in transient stability studies is an essential priority for both system planning and system operation. System planners must ascertain that the expansion plans meet the operating guidelines such as the loading of the transmission system, voltage level, etc. Usually, many stability studies might be needed for a single contingency. Operators need speed of analysis for a different reason. Operating guidelines might be needed for an unanticipated situation not studied by planners. In such situations, the operator might need the new operating guidelines in a short time.

Direct methods of transient stability offer an alternative to stability assessment by avoiding time solution. When the power system is at rest, i.e., with no disturbance, its behavior can be represented by an equilibrium solution of the differential equations. A disturbance can be viewed as the displacement of the equilibrium point from its rest position. The region of attraction of the equilibrium point is the set of points in the state-space with the property that all trajectories starting at time t_0 from a point within the set eventually converge to the equilibrium point. Direct methods attempt to obtain an approximation to the region of attraction via some mathematical function. Therefore, stability can be assessed qualitatively by determining whether the trajectory initiated by the disturbance will eventually return to the equilibrium point. Stability defined in this manner is referred to as stability in the sense of Lyapunov.

All efforts in direct methods of stability analysis are directly or indirectly related to the work of A. M. Lyapunov. The principal idea of direct method of Lyapunov is that [9] "if the rate of change of energy $E(\underline{x})$ of an isolated physical system is negative for every possible state $\underline{x}$ except for a single equilibrium state $\underline{x}_e$, then the energy will continually decrease until it finally assumes its minimum value $E(\underline{x}_e)$." This concept was formulated mathematically by Lyapunov. Since from the mathematical point of view energy cannot be defined, $E(\underline{x})$ was replaced by some scalar function $V(\underline{x})$.

Historical development of stability criteria for power systems in-

volved energy methods. The earliest energy method was the work of A. A. Gorev ("Criteria of Stability," [10]) in the 1930s, followed by Magnusson [11] in 1947, and then by Aylett [12] in 1958. In the 1960s, Lyapunov's second method was used for obtaining stability criteria. The pioneering work in this area was done by Gless [13] on a single-machine-infinite bus system, and by El-Abiad and Nagappan [14] on a multimachine system. Since then, a great amount of effort was devoted to power system stability analysis using Lyapunov's methods. The survey papers by Fouad [15] and Ribbens-Pavella [16] provide a comprehensive review of the work done in this area until the mid-1970s.

A major improvement in direct stability analysis was achieved by Athay et al. [17,18] in 1979. In previous approaches based on Lyapunov's second method, it was assumed that the most weakly coupled generators will lose synchronism irrespective of fault location. As a result, Lyapunov based methods gave conservative stability assessment for multimachine power systems. Important accomplishments of [17 and 18] are summarized here:

- A clear understanding and verification of the fact that by appropriately accounting for the fault location, the stability of a multimachine system can be accurately assessed.
- The development of the Transient Energy Stability Analysis (TESA) approach which is based on a Lyapunov theory that involves the concepts of invarient sets.
- The identification of the Potential Energy Boundary Surface (PEBS) which allows for significant improvements in direct stability assessments.

As with the previous methods of direct stability analysis, the

above TESA approach does not prove sufficiently reliable for practical application. Predictions based on an unstable equilibrium (UEP) of the fault-on trajectory often produced conservative results.

Fouad et al. [19,20,21] conducted a series of investigations in the period 1979-1981 for the purpose of dynamic security assessment via the transient energy method. A summary of some of the findings of these investigations is given below.

- The concept of the controlling (or relevant) UEP is valid.
- The critical trajectory of the critical generators is controlled by relevant UEP.
- Advanced generators in the UEP includes severely disturbed generators not losing synchronism.
- Instability is determined by the gross motion of the critical generators.
- Some transient energy, mainly a portion of the kinetic energy, does not contribute to system separation.
- For practical purposes, the critical energy is equal to the energy level at the controlling UEP.
- The transient energy margin concept is useful for assessment of the severity of disturbances; by normalizing the energy margin with respect to the kinetic energy at fault clearing a measure of the degree of stability is obtained.

These investigations showed that the Transient Energy Function (TEF) technique could accurately assess transient stability. However, further investigations were carried out in order to explain the mechanism of system separation. These effects resulted in the development of the concept of transient energy function of individual machines [22,23]. It became evident that system separation does not depend on the total system energy, but rather on the transient energy of individual machines

or groups of machines tending to separate from the rest. These concepts were also theoretically justified by the concept of partial stability and invariance principle for ordinary differential equations.

Therefore, significant progress was made in the transient stability analysis of multimachine power systems by direct methods. The progress is largely attributed to i) the development of functions that adequately describe the transient energy responsible for the separation of one or more generators from the system and ii) better estimate of the critical energy required for these generators to lose synchronism with the system. The latter issue is often referred to as the determination of the "region of stability." The problem amounts to determination of the relevant UEP among several candidates. Reference [24] has addressed this issue. A method has been given to determine the controlling UEP by accounting for two important aspects of the transient phenomena: i) the effect of the disturbance on various generators, and ii) the energy absorbing capacity of the postdisturbance network.

The transient energy function method is currently a useful technique available to power system operations planners and system planners. The TEF method has the potential of being used as an on-line technique for fast transient stability analysis. Currently, efforts are under way to automate this technique for fast stability analysis in a control center environment.

Review of Attempts to Incorporate Higher Order Models of Generator in Direct Methods

Earlier attempts to use a detailed generator model in direct methods were limited to a single machine infinite bus system [25,26]. Extension of these results to the multimachine power systems could not be achieved easily because of the nature of the nonlinearities of the augmented system. Sasaki [27] has approximately incorporated the field flux decay into transient stability of multimachine power systems by treating the field flux linkages as parameter variations. Two simplifying assumptions are made to relate the value of the internal voltage on the quadradure axis to that of voltage behind transient reactance. A Lyapunov function was obtained with values of the voltage behind transient reactance as the varying parameter. The equations describing the detailed generator model are numerically integrated for the faulted system. The critical clearing time is the time when the value of Lyapunov function along the faulted trajectory becomes equal to the critical value of the function. The critical value of the Lyapunov function is determined by the stable and unstable equilibrium points. It must be noted that the equilibrium points are dependent on the value of the varying parameter which implies that equilibrium points (the UEPs and SEPs) must be computed at the end of each time step. Therefore, practical significance of this approach is questionable when the size of the system increases beyond several generators.

Kakimoto and co-workers [28] have developed a Lyapunov function for a multimachine power system taking into account the flux decay effects, using Popov's generalized stability criterion. In this approach, in addition to certain assumptions about the nonlinearities of the system, two other key assumptions are made: a) as in [27], it is assumed that the angle between the quadrature axis and the voltage back of transient reactance is constant, and b) the transfer conductances in the reduced admittance matrix are negligible. The validity of these assumptions cannot be easily justified; particularly, the transfer conductances in the reduced admittance matrix which include the effect of the constant impedance loads.

A recent approach by Tsolas and co-workers [29] has included the flux decay effects in the direct method of transient stability analysis by using the structure preserving energy functions. The structure preserving energy functions [see 30] are based on the unreduced network formulation for the purpose of modeling nonlinear loads.

The energy function given in [29] is a function of rotor speed, rotor angle, voltage proportional to the main field winding flux linkage, and load bus voltage magnitude and phase angle.

The above attempts to include higher order models of generator in direct methods have resulted in innovative approaches and improvements in the state of the art. These attempts, however, are limited to modeling the flux decay and do not include the exciter representation. From a practical point of view, it is important to model the exciter and its effects. A mere modeling of the flux decay effects is not use-

ful for stability studies and if the exciter cannot be represented, then the classical model is a better model to use.

A very interesting idea, conceptually similar to the approach used in this dissertation, was proposed by Athay et al. [18, Chapter 6]. They used a two axis model of the generator with exciter to obtain the transient energy along the solution trajectory. Although the concepts developed in this effort were not intended to be implemented in a direct mode, interesting conclusions were drawn.

The potential energy surface was viewed as an elastic surface dependent not only on the angle-space, but also on the internal voltage-space path taken by the system. The Potential Energy Boundary Surface (PEBS) instability conjecture developed for the classical model of generator was validated in the detailed generator model fault cases.

Scope of this Project

The broad objective of this work is to improve the modeling of generator in the transient energy function method by incorporating the effect of the exciter. This is done for the purpose of first swing transient stability. The specific objectives are:

1) Obtain an energy function which includes the effect of an exciter on the first swing transient; an exciter which has a single time constant is used.

2) Obtain a practical method of evaluating the critical energy of the system for successful transient stability assessment.

3) Apply the proposed technique to the following test conditions: i) simple disturbances, ii) complex disturbances consisting of several switching operations, and iii)

determination of power transfer limit of a key generator in order to survive a three-phase fault near that generator.

4) Apply the above test conditions to practical power system models and compare the TEF results to that of time solution.

CHAPTER II. FORMULATION OF THE PROBLEM

The Two-axis Model

The two axis model of the generator has been used in this study. The derivation of this model is given in [1, Chapter 4]. In the two-axis model, the transient effects are accounted for, while the sub-transient effects are neglected. The machine is modeled by two stator circuits and two rotor circuits. The equations describing the generator are given below. In these equations, it is assumed that the direct axis leads the quadrature axis by 90 degrees.

$$\tau'_{do}\,\dot{E}'_q = E_{FD} - E'_q + (x_d - x'_d)I_d \tag{2.1}$$

$$\tau'_{qo}\,\dot{E}'_d = - E'_d - (x_q - x'_q)I_q \tag{2.2}$$

$$M\dot{\omega} = P_M - E'_d I_d - E'_q I_q + (x'_q - x'_d)I_d I_q \tag{2.3}$$

$$\dot{\delta} = \omega - 1 \tag{2.4}$$

where

E'_q	Internal generator voltage corresponding to the main field winding flux linkage
E'_d	Internal generator voltage proportional to the quadrature axis flux linkage
I_d, I_q	Projections of terminal current on generator axes
E_{FD}	Exciter output voltage (applied to generator field) converted to equivalent stator voltage
δ	Angular position of rotor quadrature axis with respect to the synchronous frame of reference

ω	The vector angular velocity with respect to the synchronous frame of reference in per unit
P_M	Generator mechanical power
τ'_{do}, τ'_{qo}	Direct and quadrature axes open-circuit transient time constants, respectively
x_d, x'_d	Synchronous and transient direct axis reactances
x_q, x'_q	Synchronous and transient quadrature axis reactances
M	Inertia constant of the generator in p.u.

Unless noted otherwise, all of the above quantities are in per unit on a 100 MVA base. For detailed description of the per unit system, see Appendix C of reference [1].

The equations describing a generator represented by classical model are:

$$M\dot{\omega} = P_M - EI_q \tag{2.5}$$

$$\dot{\delta} = \omega - 1 \tag{2.6}$$

where E is the internal generator voltage behind transient reactance. Other quantities are the same as previously defined.

If a "snapshot" of the state variables at some point in time is taken, phasor notation can be used and the relation between the internal voltages can be shown as in Figure 2.1. When the classical model of the generator is used, the voltage E'_d is zero and E' coincides with the quadrature axis. Usually, this voltage is denoted by E as defined previously. Note that the angle δ in the two-axis model represents the rotor position with respect to the synchronous frame whereas in the

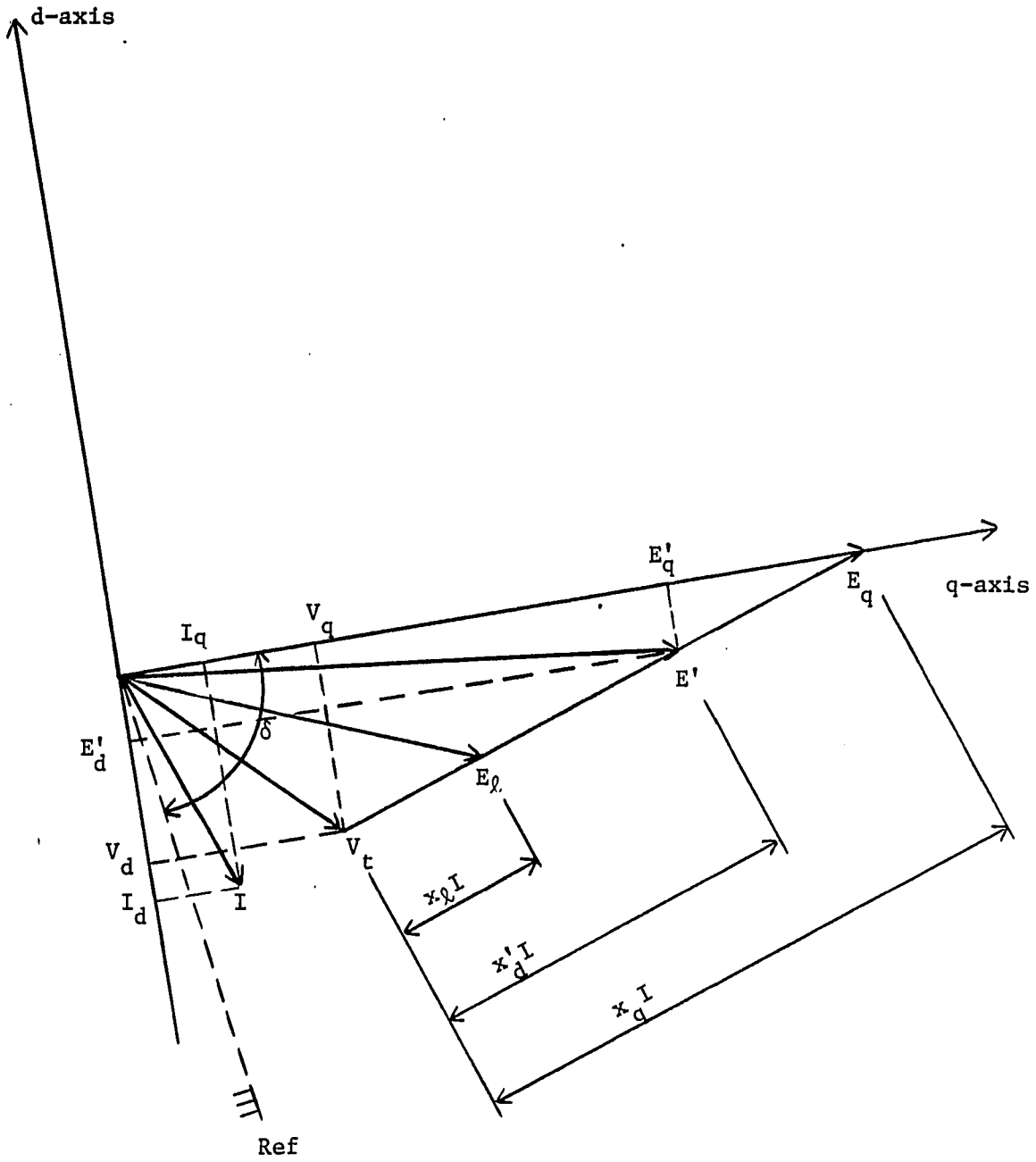

Figure 2.1. Phasor diagram of a synchronous generator

classical model the angle δ is the phase angle of the voltage behind transient reactance.

Exciter representation

The excitation system used in this study is similar to the IEEE type ST1 Potential Source Controlled-Rectifier Exciter [31]. The specific exciter used is the EPRI type G excitation system [32]. The block diagram of this exciter is given in Figure 2.2. The feedback

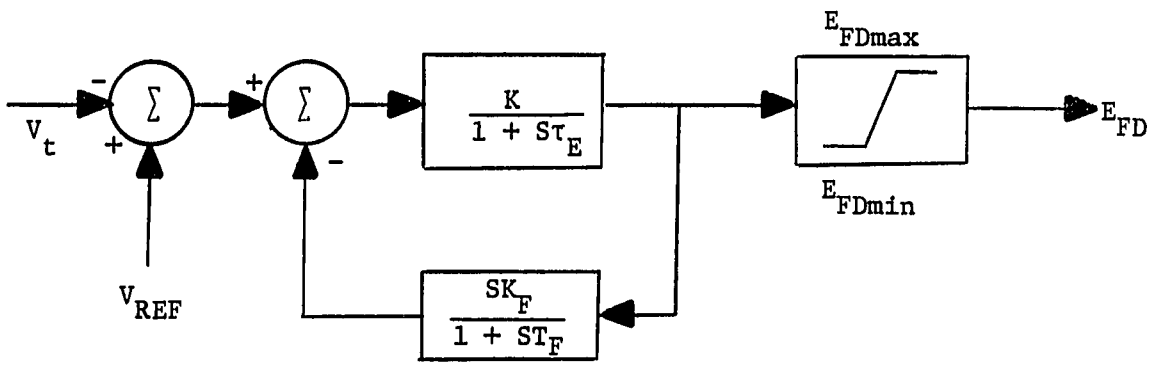

Figure 2.2. Block diagram of the type G exciter of the EPRI project RP-745

loop is a stabilizing loop which is used for transient gain reduction. The parameters K_F and T_F will be chosen so that the effect of feedback becomes negligible. In this case, the exciter can be modeled by one time constant in the forward loop.

$$\tau_E \dot{E}_{FD} = - E_{FD} + K(V_{REF} - V_t) \tag{2.7}$$

where

τ_E	The exciter time constant
E_{FDmax}, E_{FDmin}	Maximum and minimum field voltage
K	Regulator gain
V_t	Terminal voltage magnitude
V_{REF}	Reference voltage

All quantities are in per unit.

System Equations

Let there be m generators represented by the two-axis model and (n - m) generators represented by the classical model. The generators modeled in detail are equipped with the EPRI type G exciter.

$$\tau'_{d0k}\,\dot{E}'_{qk} = E_{FDk} - E'_{qk} + (x_{dk} - x'_{dk})I_{dk} \tag{2.8}$$

$$\tau'_{q_{0k}}\,\dot{E}'_{dk} = -E'_{dk} - (x_{qk} - x'_{qk})I_{qk} \tag{2.9}$$

$$\tau_{Ek}\,\dot{E}_{FDk} = -E_{FDk} - K_k(V_{REFk} - V_{tk}) \tag{2.10}$$

$$M_k\dot{\omega}_k = P_{Mk} - E'_{dk}I_{dk} - E'_{qk}I_{qk} + (x'_{qk} - x'_{dk})I_{dk}I_{qk} \tag{2.11}$$

$$\dot{\delta} = \omega_k - 1 \tag{2.12}$$

where $k = 1, 2, \ldots, m$

$$M_i\dot{\omega}_i = P_{Mi} - E_iI_{qi} \tag{2.13}$$

$$\dot{\delta}_i = \omega_i - 1 \tag{2.14}$$

where $i = m + 1, \ldots, n$.

There are 2n + 3m equations and 3n + 5m unknowns (i.e., 2n + 3m state variables, m I_ds, n I_qs and m V_ts). Therefore, n + 2m additional equations are needed to complete the description of the system. These equations are obtained from the load constraints. Therefore, the objective is to express I_d, I_q and V_t in terms of the state variables.

Consider the multimachine system shown in Figure 2.3. The network has n machines and r loads.

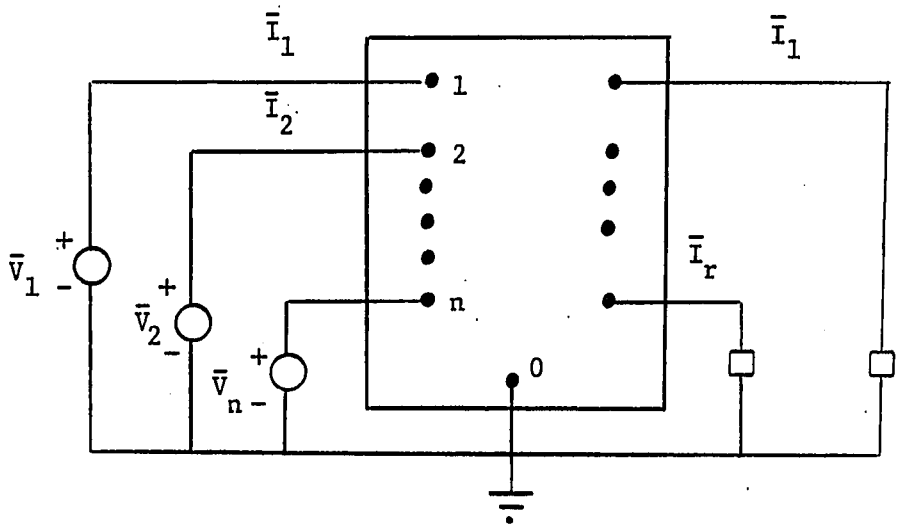

Figure 2.3. Multimachine system with constant impedance loads

The loads are assumed to be constant impedance loads. The network in Figure 2.3 can be reduced to the n-node network shown in Figure 2.4. The phasor voltages $\bar{v}_1$, ..., $\bar{v}_n$ are the internal voltages of the generators.

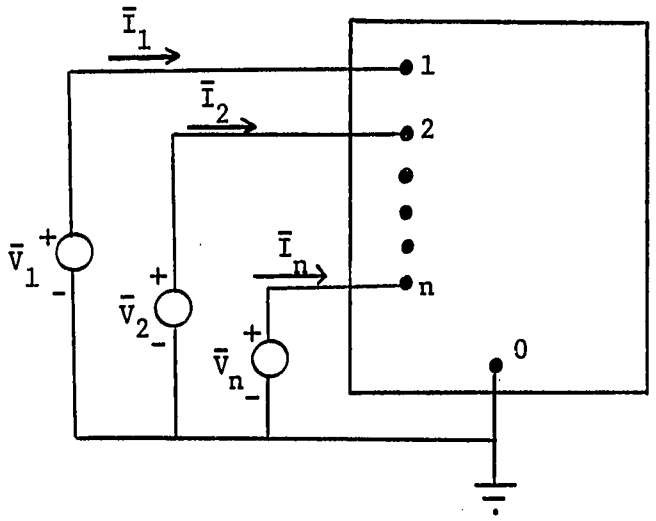

Figure 2.4. A reduced n port network

Therefore, the currents and voltages are related through

$$\begin{bmatrix} \bar{I}_1 \\ \bar{I}_2 \\ \\ \bar{I}_n \end{bmatrix} = \begin{bmatrix} \bar{Y}_{11} & \cdots & \bar{Y}_{1n} \\ \vdots & & \\ \bar{Y}_{n1} & & \bar{Y}_{nn} \end{bmatrix} \begin{bmatrix} \bar{V}_1 \\ \bar{V}_2 \\ \vdots \\ \bar{V}_n \end{bmatrix} \quad \text{or } \underline{\bar{I}} = \underline{\bar{Y}}\,\underline{\bar{V}} \qquad (2.15)$$

where $\bar{Y}_{ij} = G_{ij} + jB_{ij}$ is the ijth element of the complex admittance matrix reduced to the internal nodes of the generators. The internal voltages $\bar{V}_1, \ldots, \bar{V}_n$ are expressed in terms of reference frames that are different for each node. The current and voltage phasors can be brought to the common network frame by a simple transformation. After applying Park's transformation and the machine to network transformation, the relation between currents and voltages in direct and quadra-

ture (d-q) axis frame is of the following form [see 1, Chapter 9]:

$$\bar{\underline{I}}_{(d\text{-}q\ axis)} = (T^{-1}\bar{\underline{Y}}T)\bar{\underline{V}} \triangleq \bar{\underline{\bar{M}}}\bar{\underline{V}}_{(d\text{-}q\ axis)} \tag{2.16}$$

where

$$T_{ii} = e^{j\delta_i} \quad \text{and} \quad T_{ik} = 0 \text{ if } i \neq k.$$

The equations (2.16) can be separated into real and imaginary parts. The elements of the vector of the internal voltages, $\bar{\underline{V}}$, consist of $E'_q + jE'_d$ when the machine is modeled by the two-axis model, and $E + j0$ when the machine is represented by the classical model. Therefore, the generator k currents are given by

$$I_{qk} = \sum_{j=1}^{M} [F_{G+B}(\delta_{kj})E'_{qj} - F_{B-G}(\delta_{kj})E'_{dj}] + \sum_{\ell=m+1}^{n} F_{G+B}(\delta_{k\ell})\ E_\ell \tag{2.17}$$

$$I_{dk} = \sum_{j=1}^{m} [F_{B-G}(\delta_{kj})E'_{qj} + F_{G+B}(\delta_{kj})E'_{dj}] + \sum_{\ell=m+1}^{n} F_{B-G}(\delta_{k\ell})\ E_\ell \tag{2.18}$$

for k = 1, 2, ..., m; and

$$I_{qi} = \sum_{j=1}^{m} [F_{G+B}(\delta_{ij})E'_{qj} - F_{B-G}(\delta_{ij})E'_{dj}] + \sum_{\ell=m+1}^{n} F_{G+B}(\delta_{i\ell})\ E_\ell \tag{2.19}$$

for i = m + 1, ..., n

where

$$F_{G+B}(\delta_{rs}) \triangleq G_{rs}\mathrm{Cos}(\delta_{rs}) + B_{rs}\ \mathrm{Sin}(\delta_{rs}) \tag{2.20}$$

$$F_{B-G}(\delta_{rs}) \triangleq B_{rs} \cos(\delta_{rs}) - G_{rs} \sin(\delta_{rs}) \tag{2.21}$$

and $\delta_{rs} \triangleq \delta_r - \delta_s$.

The terminal voltage of a generator represented by the two-axis model can be related to the internal voltages by the following equations:

$$\bar{V}_{tk} = V_{qk} + jV_{dk} , \quad V_{tk} = (V_{qk}^2 + V_{qk}^2)^{1/2} \tag{2.22}$$

$$V_{qk} = E'_{qk} + x'_{dk} I_{dk} \tag{2.23}$$

$$V_{dk} = E'_{dk} - x'_{qk} I_{qk} \tag{2.24}$$

for k = 1, 2, ..., m.

Equations 2.23 and 2.24 are inconsistent with the model assumed in equation 2.15. Consider the kth generator in Figure 2.4; this is shown in Figure 2.5.

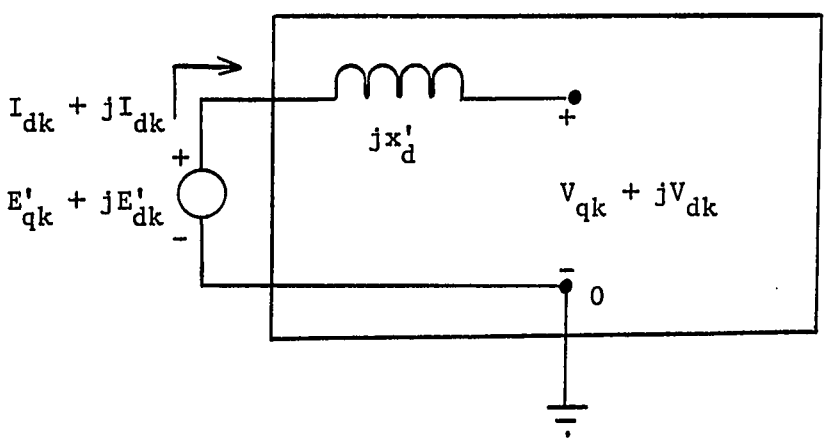

Figure 2.5. Representation of generator k in a multi-machine network

Figure 2.5 implies that

$$V_{qk} = E'_{qk} + x'_{dk} I_{dk} \tag{2.25}$$

$$V_{dk} = E'_{dk} - x'_{dk} I_{qk} \tag{2.26}$$

Since normally x'_d and x'_q are close, it will be assumed that $x'_d = x'_q$.

Therefore, the differential equations 2.8-2.14 and algebraic equations 2.17-2.19, 2.22, and 2.25, 2.26 completely describe the system. Next, these equations will be transformed to the center of inertia frame of reference.

Transformation to the center of inertia (COI)

In order to obtain a convenient expression for the energy function, the angles and speeds must be transformed to their center of inertia. Using equations 2.11, 2.12, 2.13, and 2.14, the procedure is as follows:

$$\sum_{j=1}^{n} M_j \dot{\omega}_j = \sum_{j=1}^{n} P_{Mj} - \sum_{k=1}^{m} [E'_{dk} I_{dk} + E'_{qk} I_{qk} - (x'_{qk} - x'_{dk}) I_{dk} I_{qk}]$$

$$- \sum_{i=m+1}^{n} E_i I_{qi}$$

$$\triangleq P_{COI} \triangleq M_T \dot{\omega}_0 \tag{2.27}$$

where

$$M_T \triangleq \sum_{j=1}^{n} M_j$$

Therefore,

$$\dot{\omega}_0 = \frac{1}{M_T} P_{COI}. \tag{2.28}$$

Also,

$$\delta_0 = \frac{1}{M_T} \sum_{j=1}^{n} M_j \delta_j \tag{2.29}$$

which implies

$$\begin{aligned} \dot{\delta}_0 &= \frac{1}{M_T} \sum_{j=1}^{n} M_j \dot{\delta}_j \\ &= \frac{1}{M_T} \sum_{j=1}^{n} M_j (\omega_j - 1). \end{aligned} \tag{2.30}$$

Define

$$\tilde{\omega}_j \triangleq \omega_j - \omega_0 \tag{2.31}$$

$$\theta_j \triangleq \delta_j - \delta_0 \tag{2.32}$$

which implies

$$\dot{\tilde{\omega}}_j = \dot{\omega}_j - \dot{\omega}_0 \tag{2.33}$$

$$\dot{\theta}_j = \dot{\delta}_j - \dot{\delta}_0 \tag{2.34}$$

for j = 1, 2, ..., n.

$$\dot{\tilde{\omega}}_k = \dot{\omega}_k - \dot{\omega}_0 = \frac{1}{M_k}[P_{Mk} - E'_{dk}I_{dk} - E'_{qk}I_{qk} + (x'_{qk} - x'_{dk})I_{dk}I_{qk}]$$

$$- \frac{1}{M_T} P_{COI} \tag{2.35}$$

Therefore, for machines represented by the two-axis model the swing equation in the COI frame is

$$M_k\dot{\tilde{\omega}}_k = P_{Mk} - E'_{dk}I_{dk} - E'_{qk}I_{qk} + (x'_{qk} - x'_{dk})I_{dk}I_{qk} - \frac{M_k}{M_T} P_{COI} \tag{2.36}$$

for k = 1, 2, ..., m.

Similarly,

$$M_i\dot{\tilde{\omega}}_i = P_{Mi} - E_iI_{qi} - \frac{M_i}{M_T} P_{COI} \tag{2.37}$$

for i = m + 1, ..., n.

$$\dot{\delta}_j - \dot{\delta}_0 = (\omega_j - 1) - \frac{1}{M_T}\sum_{\ell=1}^{n} M_\ell(\omega_\ell - 1)$$

$$= \omega_j - 1 - \frac{1}{M_T}\sum_{\ell=1}^{n} M_\ell\omega_\ell + \frac{1}{M_T}\sum_{\ell=1}^{n} M_\ell$$

$$= \omega_j - 1 - \omega_0 + 1$$

$$= \omega_j - \omega_0$$

$$= \tilde{\omega}_j$$

Therefore,

$$\dot{\theta}_j = \tilde{\omega}_j \qquad \text{where } j = 1, 2, \ldots n \tag{2.38}$$

The rest of equations describing the system remain unchanged because angles appear only in the form of $\delta_i - \delta_j$ and

$$\theta_{ij} \triangleq \theta_i - \theta_j$$

$$= (\delta_i - \delta_0) - (\delta_j - \delta_0)$$

$$= \delta_i - \delta_j \triangleq \delta_{ij} .$$

The complete set of equations describing the system in the center of inertia are listed here with the assumption that $x'_d = x'_q$.

$$\tau'_{d0k} \dot{E}'_{qk} = E_{FDk} - E'_{qk} + (x_{dk} - x'_{dk}) I_{dk} \tag{2.39}$$

$$\tau'_{q0k} \dot{E}'_{dk} = - E'_{dk} - (x_{qk} - x'_{dk}) I_{qk} \tag{2.40}$$

$$\tau_E \dot{E}_{FDk} = - E_{FD} + K_k (V_{REFk} - V_{tk}) \tag{2.41}$$

$$M_k \dot{\tilde{\omega}}_k = P_{Mk} - E'_{dk} I_{dk} - E'_{qk} I_{qk} - \frac{M_k}{M_T} P_{COI} \tag{2.42}$$

$$\dot{\theta}_k = \tilde{\omega}_k \tag{2.43}$$

$$I_{qk} = \sum_{j=1}^{m} [F_{G+B}(\theta_{kj})E'_{qj} - F_{B-G}(\theta_{kj})E'_{dj}] + \sum_{\ell=m+1}^{n} F_{G+B}(\theta_{k\ell})E_{\ell} \tag{2.44}$$

$$I_{dk} = \sum_{j=1}^{m} [F_{B-G}(\theta_{kj})E'_{qj} - F_{B-G}(\theta_{kj})E'_{dj}] + \sum_{\ell=m+1}^{n} F_{B-G}(\theta_{k\ell})E_{\ell} \tag{2.45}$$

$$V_{tk} = (V_{qk}^2 + V_{dk}^2)^{1/2} \tag{2.46}$$

$$V_{qk} = E'_{qk} + x'_{dk} I_{dk} \tag{2.47}$$

$$V_{dk} = E'_{dk} - x'_{dk} I_{dk} \tag{2.48}$$

where k = 1, 2, ..., m.

$$M_i \dot{\tilde{\omega}}_i = P_{Mi} - E_i I_{qi} - \frac{M_i}{M_T} P_{COI} \tag{2.49}$$

$$\dot{\theta}_i = \tilde{\omega}_i \tag{2.50}$$

$$I_{qi} = \sum_{j=1}^{m} [F_{G+B}(\theta_{ij})E'_{qj} - F_{B-G}(\theta_{ij})E'_{dj}] + \sum_{\ell=m+1}^{n} F_{G+B}(\theta_{i\ell})E_{\ell} \tag{2.51}$$

where i = m + 1, ..., n.

$$F_{G+B}(\theta_{rs}) = G_{rs} \cos(\theta_{rs}) + B_{rs} \sin(\theta_{rs}) \tag{2.52}$$

$$F_{B-G}(\theta_{rs}) = B_{rs} \cos(\theta_{rs}) - G_{rs} \sin(\theta_{rs}) \tag{2.53}$$

$$P_{COI} = \sum_{j=1}^{n} P_{Mj} - \sum_{k=1}^{m} [E'_{dk} I_{dk} + E'_{qk} I_{qk}] - \sum_{i=m+1}^{n} E_i I_{qi} \tag{2.54}$$

CHAPTER III. UNSTABLE EQUILIBRIUM POINTS

The Inertial Effects

Transient stability is the problem of the performance of the power system under severe disturbances. The primary concern in transient stability study is the first swing transient. The important factors that affect the performance of the power system during the first swing transient are [1, Chapter 8, 2, and 6]:

1) The type of disturbance, its location and duration.
2) The "strength" of the power network to provide synchronizing torques during the transient.
3) The turbine-generator parameters.

The system parameters that affect the above factors are (a) the inertia constant, (b) the direct axis transient reactance, (c) the direct axis open circuit time constant, and (d) the excitation system.

To observe the effect of some of the above factors, consider the block diagram of Figure 3.1, where a generator is represented by a single time constant, and equipped with an exciter. This block diagram shows a generator at no load.

Any change in the terminal voltage, V_t, from the reference voltage, V_{REF}, provides an error signal to the excitation system. But there is a major delay in the feedback loop of Figure 3.1 due to the effective value of τ'_{d0} when the generator is loaded. Kimbark [33] shown that under load the effective value of the direct axis time constant is lower than τ'_{d0}. A typical value of this effective time

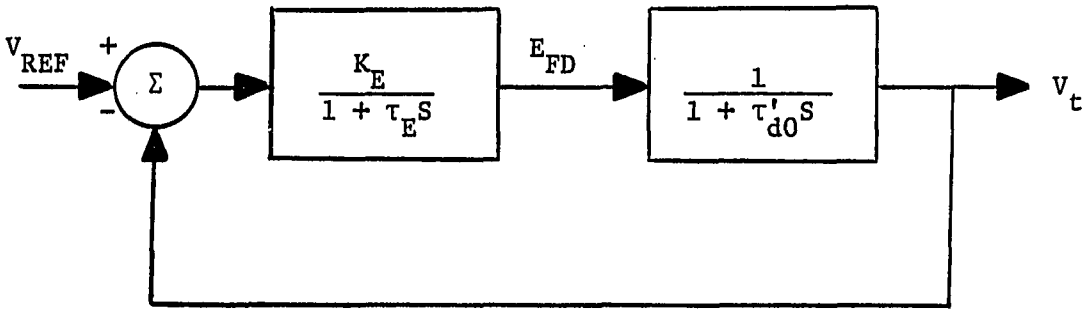

Figure 3.1. Block diagram of a generator with exciter

constant is about two seconds [1].

Therefore, regardless of the quickness of the excitation system the generator parameters determine the initial dynamic response to the disturbance.

Suppose the disturbance is initiated by a fault. The excitation systems of the generators close to the fault location influence the first swing transient by increasing the internal flux of these generators which, in turn, causes an increase in the electrical power output. In other words, the role of exciter is in "strengthening" the synchronizing forces of the system during the transient. However, the characteristics of the dynamic response is dictated by the kinetic energy stored in the rotating masses.

Observation of the generator behavior indicates that the state variables that are mainly influenced by the inertial effects, namely, the rotor angles θ, are the dominant state variables. Thus, the

concepts of unstable equilibrium points and mode of disturbance (M.O.D.) developed for the classical model can be extended to the present formulation.

State Space Formulation for Computing Equilibrium Points

The equations (2.38-2.53) of Chapter II describe a system of n - m machines represented by the classical model, and m machines, equipped with exciters, represented by the two-axis model. These equations can be written in vector form

$$\dot{\underline{x}} = \underline{f}(\underline{x}) \tag{3.1}$$

where

$\underline{x}^t = [\underline{x}_1^t, \underline{x}_2^t, \underline{x}_3^t, \underline{x}_4^t, \underline{x}_5^t]$ is the vector of state variables.

$$\begin{aligned}
\underline{x}_1^t &= [E'_q, \ldots, E'_{qm}] \\
\underline{x}_2^t &= [E'_{d1}, \ldots, E'_{dm}] \\
\underline{x}_3^t &= [E_{FD1}, \ldots, E_{FDm}] \\
\underline{x}_4^t &= [\theta_1, \ldots, \theta_m] \\
\underline{x}_5^t &= [\theta_{m+1}, \ldots, \theta_n] \\
\underline{f}^t(\underline{x}) &= [\underline{f}_{k1}, \underline{f}_{k2}, \underline{f}_{k3}, \underline{f}_{k4}, \underline{f}_{k5}]
\end{aligned} \tag{3.2}$$

where

$$f_{k1} = \frac{1}{\tau'_{d0k}} [E_{FDk} - E'_{qk} + (x_{dk} - x'_{dk})I_{dk}] \tag{3.3}$$

$$f_{k2} = \frac{1}{\tau'_{q_{0k}}} [- E'_{dk} - (x_{qk} - x'_{dk})I_{qk}] \tag{3.4}$$

$$f_{k3} = g(F_{FDk}, V_{tk}, V_{REFk}, K_k) \tag{3.5}$$

$$f_{k4} = \frac{1}{M_k} [P_{Mk} - E'_{dk}I_{dk} - E'_{qk}I_{qk} - \frac{M_k}{M_T} P_{COI}] \tag{3.6}$$

$$f_{k5} = \frac{1}{M_\ell} [P_{M\ell} - E_\ell I_{q\ell} - \frac{M_\ell}{M_T} P_{COI}] \tag{3.7}$$

where

k1 = k = 1, 2, ..., m

k2 = m + 1, ..., 2m

k3 = 2m + 1, ..., 3m

k4 = 3m + 1, ..., 4m

k5 = 4m + 1, ..., n + 3m - 1

ℓ = m + 1, ..., n - 1

Although n + 3m equations describe the system, this is not the minimal order because one of the angles, assume θ_n without loss of generality, is dependent on the rest of the angles. Therefore, n + 3m - 1 equations is the minimal order.

The equilibrium points of system (3.1) are given by the solutions of

$$\dot{\underline{x}} = \underline{f}(\underline{x}) = \underline{0}. \tag{3.8}$$

Usually, within a periodic frame of rotor angles there is one stable equilibrium point and a number of unstable equilibrium points. Digression will be made here to discuss the unstable equilibrium points of a system represented by the classical model.

Consider a power system of r generators represented by the classical model. The equations describing this system in the inertial center frame are similar to (2.49 - 2.50). The equilibrium points of this system are the solutions of

$$\dot{\underline{y}} = \underline{g}(\underline{y}) = \underline{0} \tag{3.9}$$

where $\underline{y}$ is the vector of angles $\underline{\theta}$ and speeds $\underline{\tilde{\omega}}$ for the r generators in the system. For the postdisturbance situation, equations (3.9) generally have one stable equilibrium point and many (depending on the size of the system) unstable equilibrium points. The vector of unstable equilibrium points contains one or more elements with angles $\theta^U > \pi/2$ [14-16]. For a given disturbance, there is a critical group of generators which are most severely disturbed [19-21]. They are the generators whose angles are advanced; they form the Mode of Disturbance (M.O.D.) previously known as the Mode of Instability. The generators which belong to M.O.D. usually have $\theta^U > \pi/2$.

Solution Method and the Numerical Aspects

The equilibria of (3.8) can be found by casting the problem into a least-squares problem. In other words, the equilibria of (3.8) are

the local minima of the objective function defined by:

$$F(\underline{x}) \triangleq \sum_{i=1}^{n+3m} f_i^2(\underline{x}) \tag{3.10}$$

Since the local minima must be zero, the problem becomes that of solving

$$F(\underline{x}) = 0. \tag{3.11}$$

The solution technique used for solving (3.11) was a modified form of Newton-Raphson technique as outlined below:

1) Start with an initial guess $\hat{\underline{x}}$.

2) Find the gradient of F from

$$\underline{g}(\underline{x}^r) = 2J^t\underline{f}(x^r)$$

where

$\underline{x}^r$ is the vector of state variables at the rth iteration.

$\underline{g}(\underline{x}^r)$ is the $(n + 3m - 1) \times (n + 3m - 1)$ gradient vector evaluated at $\underline{x} = \underline{x}^r$.

$\underline{f}(\underline{x}^r)$ is found from (3.3-3.7) evaluated at $\underline{x} = x^r$.

J^t is the transpose of the jacobian matrix evaluated at $\underline{x} = \underline{x}^r$. The elements of J are the partial derivatives of elements of $\underline{f}$ with respect to the elements of $\underline{x}$. J is of size $(n + 3m - 1) \times (n + 3m - 1)$.

3) Find the direction of search from

$$\underline{P}(\underline{x}) = - \underline{g}(\underline{x})$$

4) Update the value of $\underline{x}$

$$\underline{x}^{r+1} = \underline{x}^r + 1\underline{P}(\underline{x}^r) \qquad \text{(simple Newton-Raphson step)}$$

5) Compute $F(x^r)$ and $F(x^{r+1})$. If $F(x^{r+1}) < F(x)$, i.e., if the objective function decreases, this is an indication that the step taken was in a descent direction; so continue with the step size of unity and go to step 2 if the solution has not yet been found.

   If $F(x^{r+1}) > F(x^r)$ then the step taken was not in the descent direction. There is a need for an optimum direction of search. Go to step 6.

6) Optimum direction of search is computed from one-dimensional minimization along a certain direction of search:

$$\min F(\underline{x}^r + \alpha^{(r)} \underline{P}(\underline{x}^r))$$

   where minimization is over α; and $\underline{x}^{(r)}$ is held fixed. Cubic interpolation is used for this minimization. The objective is to find α^* which minimizes $F(\underline{x}^r + \alpha^{(r)} \underline{P}(\underline{x}^r))$.

7) Update the value of $\underline{x}^r$

$$\underline{x}^{r+1} = \underline{x}^r + \alpha^* \underline{P}(x^r)$$

8) Compute the new objective function and test whether solution has been found. If not, go to step 2.

The procedure outlined above is used to determine the stable or unstable equilibrium points of the system described by (3.1). Post-disturbance stable equilibrium points can be found by using the pre-fault values (determined from loadflow study) as the starting point. The algorithm usually converges very rapidly to the solution.

For finding the Unstable Equilibrium points (UEPs), the procedure outlined below is followed.

1) The postdisturbance admittance matrix reduced to the internal nodes of the generators is computed.

2) The prefault value of all of the state variables is obtained.

3) Assuming that the mode of disturbance is known, the corner points are computed. If machines i, j, ..., r belong to the mode of disturbance, the starting value for the rotors of these machines are $\pi-\theta_i^s$, $\pi-\theta_j^s$, ..., $\pi-\theta_r^s$ where θ^s's can be either prefault stable equilibrium points or the postfault stable equilibrium points. The starting values for the rest of the state variables are the prefault or the postfault stable equilibrium points.

This procedure has been implemented and the results are given in Chapters V and VI.

The Newton-Raphson method employed here has similar advantages and disadvantages observed in other Newton methods. Usually, convergence is rapid, but is not guaranteed; sometimes, the algorithm fails to converge to the UEP.

Exciter Reference Voltage

Prior to the initiation of the disturbance, the system is at steady-state and the equations (3.8) must be satisfied. From the loadflow study, values of P_M, V_t and δ are known. Therefore, the initial values of E'_q, and E'_d can be easily computed. The initial value of E_{FD}, E_{FD}^0, is selected such that equation (3.3) is zero in the prefault state.

For exciter type G described in Chapter II, equation (3.5) becomes:

$$f_{k3} = \frac{1}{\tau_{Ek}} [- E_{FDk} + K_k(V_{REFk} - V_{tk})]. \qquad (3.12)$$

In order to have $f_{k3} = 0$ in the prefault state, the reference voltage

can be computed according to

$$V_{REFk} = (E^0_{FDk}/K_k) + V^0_{tk} \tag{3.13}$$

where the superscript 0 denotes the prefault conditions.

Modeling the Limiter on the Exciter

Consider equations (3.3) and (3.12) repeated here.

$$f_{k1} = \frac{1}{\tau'_{d0k}} [E_{FDk} - E'_{qk} + (x_{dk} - x'_{dk})I_{dk}] \tag{3.3}$$

$$f_{k3} = \frac{1}{\tau_{Ek}} [- E_{FDk} + K_k(V_{REF} - V_{tk})] \tag{3.12}$$

Equation (3.12) represents the exciter without the limiter. Therefore, the value of E_{FDk} in (3.12) can assume any value to satisfy the condition $f_{k3} = 0$. The value of E_{FDk} used in (3.3) is the output of the exciter, thus this value is bounded by the limiter on the exciter.

Therefore, if the value of E_{FDk} exceeds the limit, the constant limit value must be used for E_{FDk} in (3.3). As a result, the contribution of E_{FDk} in equation (3.3) to the Jacobian matrix is zero.

CHAPTER IV. ENERGY FUNCTION

The Basic Approach

The approach taken for obtaining an energy function is based on the method of first integrals. This method is a technique used to study conservative systems in classical mechanics [34]. The first integral of a system represented by differential equations $\dot{\underline{x}} = \underline{f}(\underline{x})$ is a differentiable function $V(\underline{x})$ defined over a domain D of the state space such that for a solution $\underline{x}$, $V(\underline{x})$ assumes a constant value C.

For the classical model representation of a power system, the energy function is obtained as the first integral of the swing equations as follows:

$$V(\tilde{\underline{\omega}}, \underline{\theta}) = \sum_{i=1}^{r} \int (M_i \dot{\tilde{\omega}}_i - P_{ai})\, \tilde{\omega}_i dt$$

$$V(\tilde{\underline{\omega}}, \underline{\theta}) = \sum_{i=1}^{r} \int M_i \tilde{\omega}_i d\tilde{\omega}_i + \sum_{i=1}^{r} \int (-P_{ai}) d\theta_i \qquad (4.1)$$

where

$\tilde{P}_{ai} \triangleq P_{Mi} - P_{ei}$ is the accelerating power.

The first term in (4.1) corresponds to the kinetic energy of the system and the second term is the potential energy.

Similarly, for the detailed representation the energy function will be formulated as the first integral of the balance of power equations. However, the difficulty in evaluating the transient energy is that some of the components of the potential energy are path-dependent

integrals and a closed-form solution for the resulting integrals cannot be found unless some simplifying assumptions or approximations are made. Depending on the assumptions made, three different energy formulations will be given and analyzed.

Terminal Voltage Formulation

Let $\bar{V}_i = V_i \angle \beta_i$ be the terminal voltage for machines represented in detail. Note that β_i must be computed with respect to the center of inertia (COI) of the rotor angles. With the admittance matrix reduced to the internal nodes of machines represented by the classical model, and the terminal voltage nodes of the machines represented in

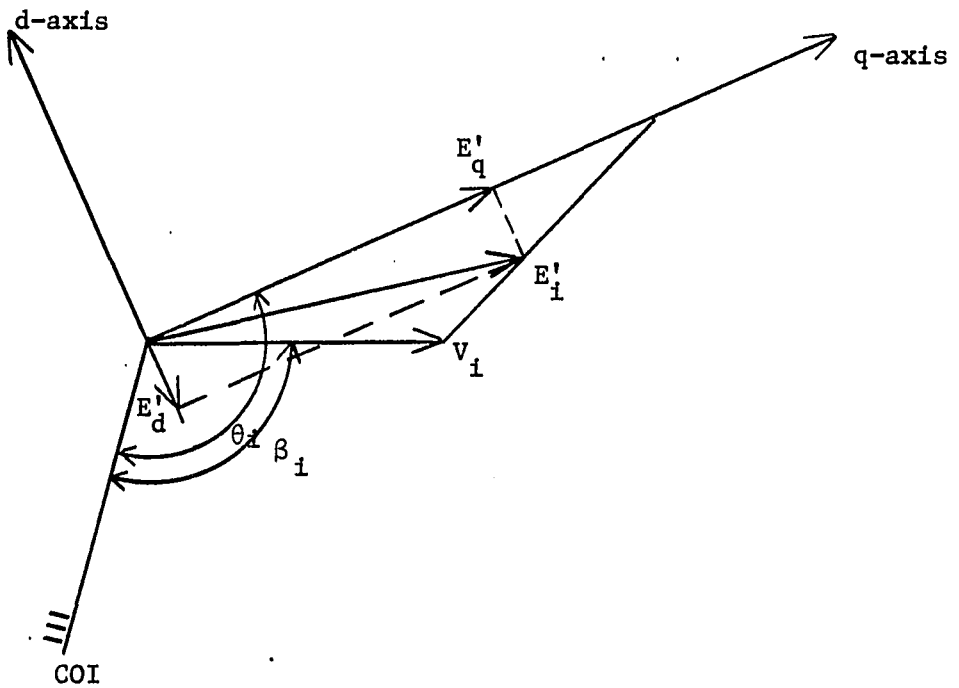

Figure 4.1. Phasor diagram for terminal voltage formulation

detail, the swing equation is of the form:

$$\dot{M_i\tilde{\omega}_i} = P_{Mi} - [V_i^2 G'_{ii} + \sum_{\substack{j=1 \\ j\neq i}}^{n} V_i V_j (B'_{ij} \text{ Sin } \beta_{ij} + G'_{ij} \text{ Cos } \beta_{ij})]$$

$$- \frac{M_i}{M_T} P_{COI} , \qquad i = 1, 2, \ldots, n \tag{4.2}$$

where G'_{ij} and B'_{ij} are the real and imaginary parts of the elements of of the y-matrix described above, and V is either the terminal voltage or internal voltage.

In equation (4.2), V must be replaced with E and β with θ when i or j belong to the set of machines represented by the classical model.

The kinetic energy is given by:

$$V_{KE} = \int \sum_{i=1}^{n} M_i \dot{\tilde{\omega}}_i \tilde{\omega}_i dt$$

$$= \sum_{i=1}^{n} \int M_i \tilde{\omega}_i d\tilde{\omega}_i$$

$$= \sum_{i=1}^{n} \frac{1}{2} M_i \tilde{\omega}_i^2 \tag{4.3}$$

The potential energy is:

$$V_{PE} = - \int_{\theta_i^{cl}}^{\theta_i} \sum_{i=1}^{n} P_{ai} d\theta_i , \qquad \theta_i^{cl} = \theta_i \text{ at fault clearing}$$

$$= - \sum_{i=1}^{n} P_{Mi} (\theta_i - \theta_i^{cl}) + \sum_{i=1}^{n} \int_{\theta_i^{cl}}^{\theta_i} G'_{ii} V_i^2 d\theta_i$$

$$+ \sum_{i=1}^{n-1} \sum_{j=i+1}^{n} \left[\int_{\theta_{ij}^{cl}}^{\theta_{ij}} B'_{ij} V_i V_j \, \mathrm{Sin}\beta_{ij} \, d\theta_{ij} \right.$$

$$\left. + \int_{\theta_i^{cl}+\theta_j^{cl}}^{\theta_i+\theta_j} G'_{ij} V_i V_j \, \mathrm{Cos}\beta_{ij} \, d(\theta_i + \theta_j) \right] \qquad (4.4)$$

Note that

$$\sum_{i=1}^{n} \int_{\theta_i^{cl}}^{\theta_i} \frac{M_i}{M_T} P_{COI} \, d\theta_i = 0$$

because $\sum_{i=1}^{n} M_i \theta_i = 0.$

To evaluate the above integrals, the following assumptions are made:

For machines represented in detail,

- β_i is linearly related to θ_i
- V_i is linearly related to θ_i

The derivation of the energy function is given in Appendix A. Time simulation studies were made to study the validity of the assumptions. In general, the assumptions cannot be well justified. Figures 4.2 and 4.3 show the plot of terminal voltage vs. angle θ for generators 9 and 10 of the BC Hydro system for a fault at WSN500 (see Chapter V).

A variation of this formulation is to assume constant terminal voltage. This assumption is plausible because an ideal excitation sys-

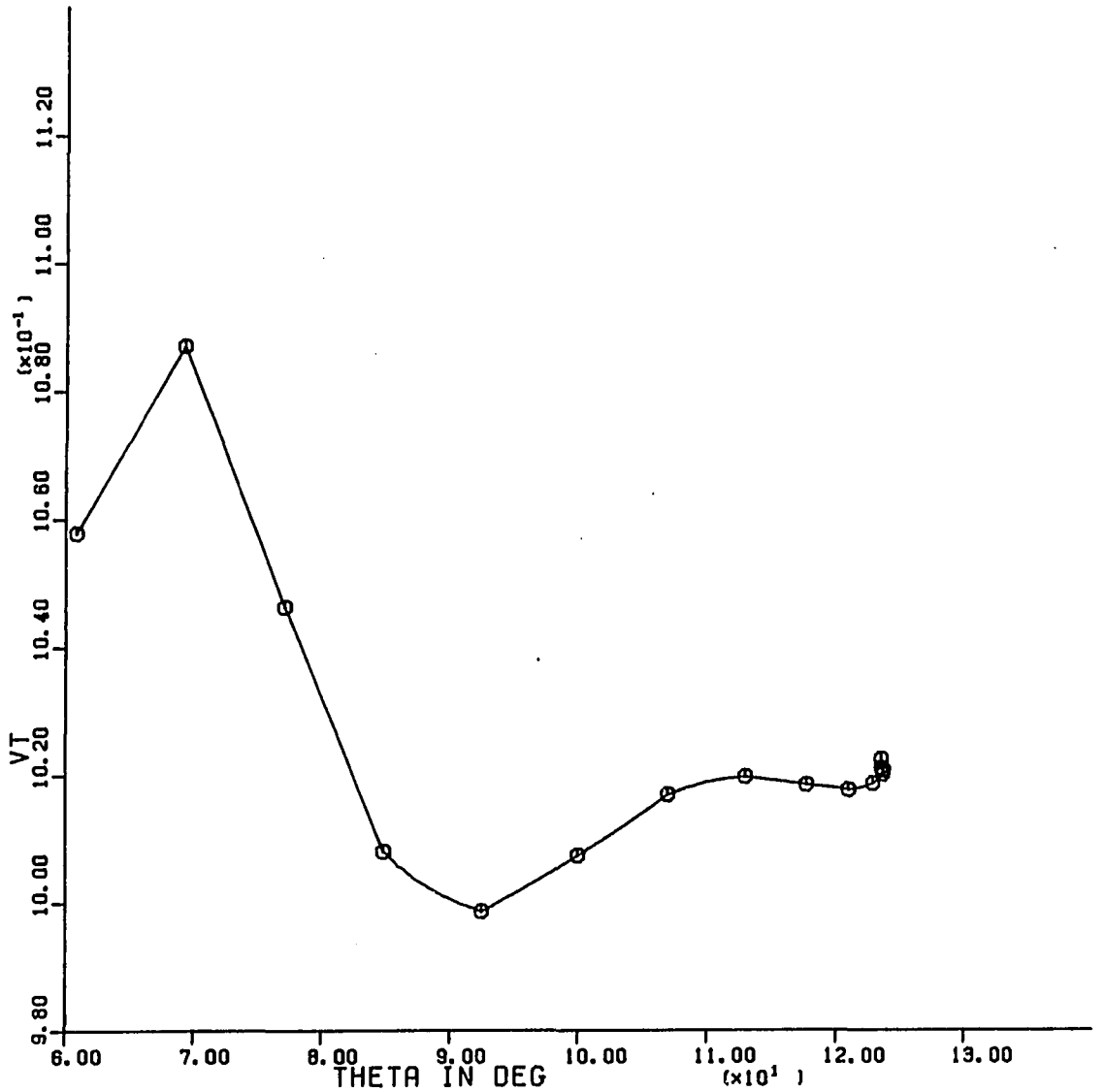

Figure 4.2. Variation of terminal voltage with angle θ for generator #9

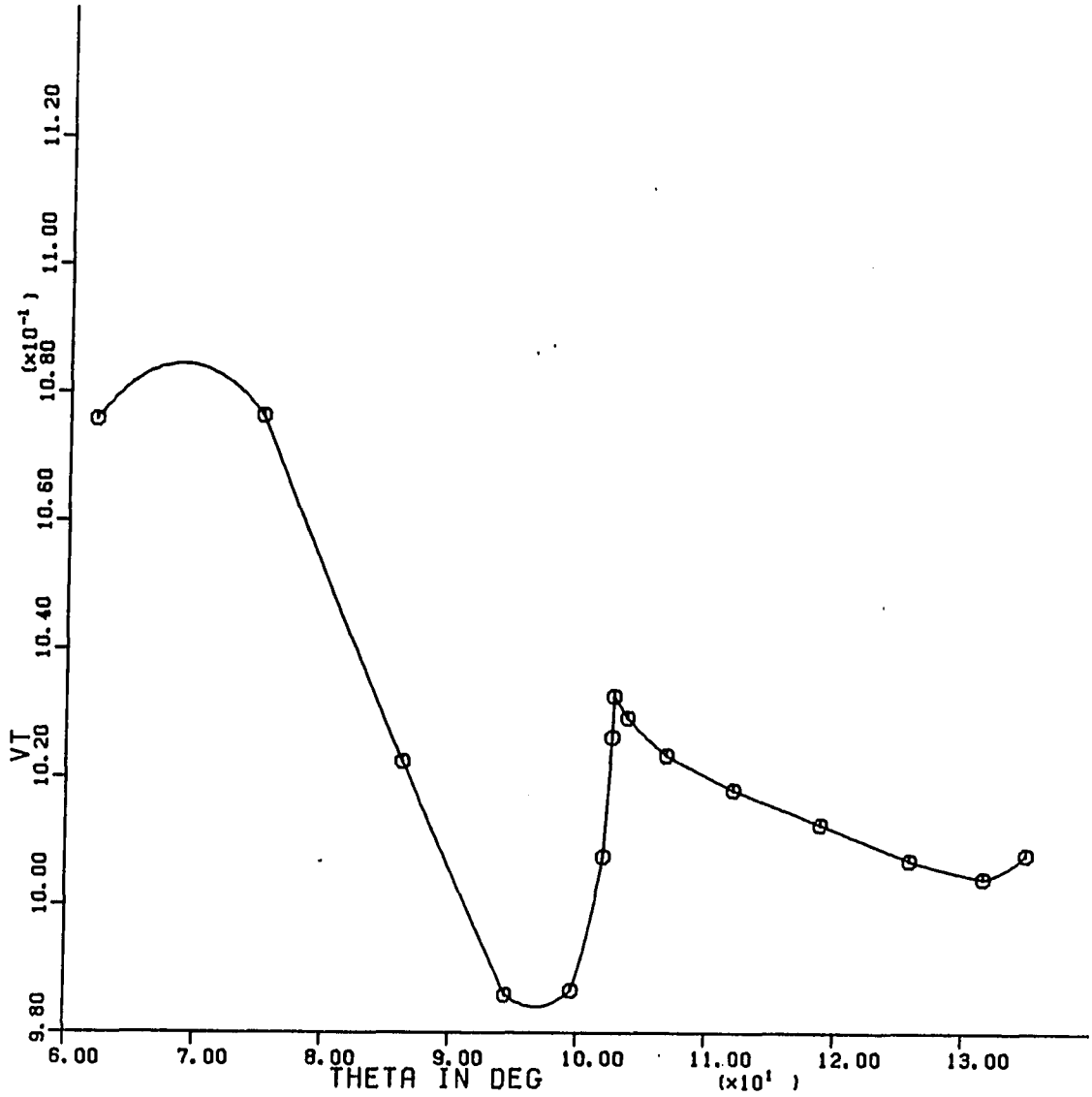

Figure 4.3. Variation of terminal voltage with angle θ for generator #10

tem must maintain constant terminal voltage. However, for evaluating the integrals in (4.4), a relation between β_i and θ_i are still required. This approach was not pursued further.

E' Formulation

Consider a generator represented by the two-axis model. Viewed from the terminal node, the generator can be represented by a variable voltage source behind transient reactance x'_d (Figure 4.4). In phasor notation, the relation among variables is shown in Figure 4.5.

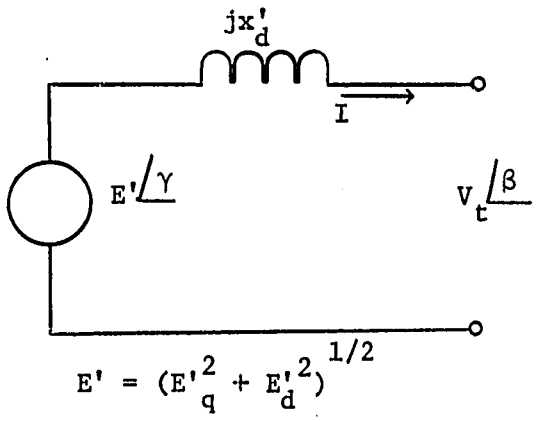

Figure 4.4. A variable voltage source behind transient reactance

The swing equation is given by:

$$M_i\dot{\tilde{\omega}}_i = P_{Mi} - [E'^2_i G_{ii} + \sum_{\substack{j=1 \\ j\neq i}}^{n} E'_i E'_j (B_{ij} \text{ Sin } \gamma_{ij} + G_{ij} \text{ Cos } \gamma_{ij})] - \frac{M_i}{M_T} P_{COI} \qquad (4.5)$$

where E' and γ are replaced by E and θ when i or j belong to the set of

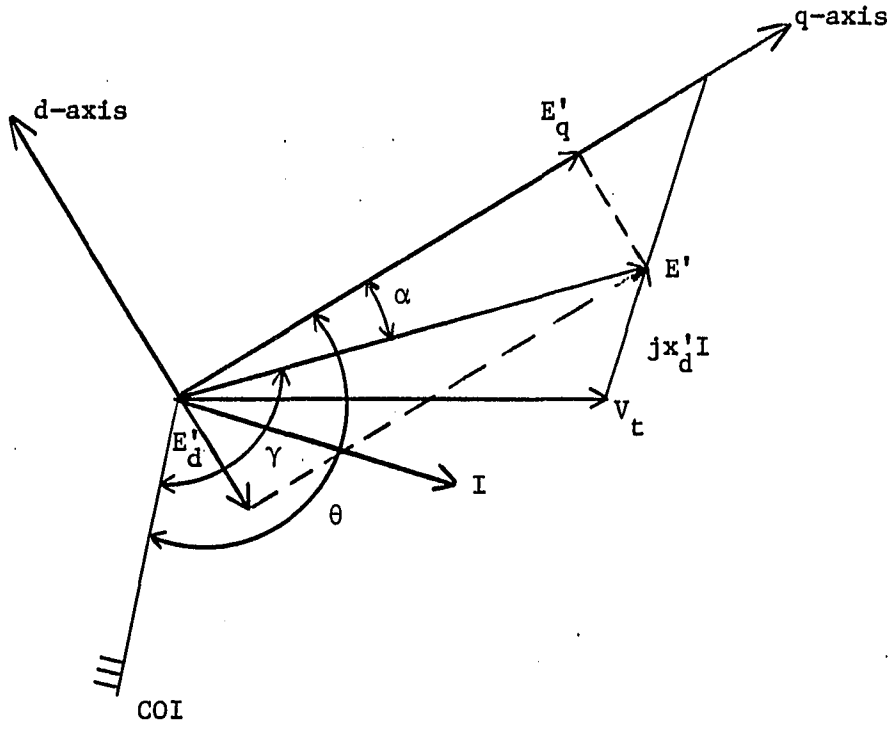

Figure 4.5. Phasor diagram of Figure 4.4

generators represented by the classical model.

The energy function can be defined in the space of angles γ by multiplying (4.5) by $d\gamma_i/dt$, summing over all i, and integrating with respect to time. The change in potential energy involves the following integrals:

$$\Delta V_{PE} = \sum_{i=1}^{n} (I_{PMi} + I_{Pi}) + \sum_{i=1}^{n-1} \sum_{j=i+1}^{n} (I_{sij} + I_{cij}) \qquad (4.6)$$

where

$$I_{PMi} = - P_{Mi}(\gamma_i - \gamma_i^{cl})$$

$$I_{Pi} = G_{ii} \int_{\gamma_{i}^{cl}}^{\gamma_i} E_i'^{2} \, d\gamma_i$$

$$I_{Sij} = B_{ij} \int_{\gamma_{ij}^{cl}}^{\gamma_{ij}} E_i' E_j' \sin\gamma_{ij} \, d\gamma_{ij}$$

$$I_{Cij} = C_{ij} \int_{\gamma_i^{cl}+\gamma_j^{cl}}^{\gamma_i+\gamma_j} E_i' E_j' \cos\gamma_{ij} \, d(\gamma_i + \gamma_j)$$

The internal voltage E' is related to the flux linking the d and q-axis windings and these, in turn, are related to the excitation level. For a disturbance such as a fault, a fast excitation system will raise the flux level, particularly the flux linking the main field winding, during the period that angular position of rotor reaches a maximum. Therefore, in the time period in which the first swing reaches its peak, the rotor position of the critical machines and the corresponding internal voltages, E', increase monotonically. During this period, the internal voltage E' can reasonably be modeled by

1) A constant value representing the average value of change of E' within two extremes, or

2) a linear function of θ.

Determining the value of E' for either of the assumptions will be explained in the following sections.

Constant E'

Modeling E' by a constant average value, the integrals in (4.6) can be evaluated. Using this assumption, the form of integrals are

identical to those of the classical model with the exception that integration is with respect to angles γ.

The drawback of this formulation is that the kinetic and potential energy are functions of the variables γ and $\dot{\gamma}$ rather than θ and $\tilde{\omega}$. An additional problem is that $\sum_{i=1}^{n} \int \frac{M_i}{M_T} P_{COI} \, d\gamma_i$ is nonzero and must be evaluated. Evaluation of this integral would be an added computational burden.

Linear E'

To remove the difficulties associated with integration with respect to γ, a variation of the E' formulation can be obtained by assuming the angle α (see Figure 4.5) to remain constant during the post-disturbance period. In reference [27], a similar assumption is made. Normally, the changes in angles α are not great compared to rotor angles θ. The value of α can be assumed to remain fixed at the fault clearing value.

An energy function has been obtained (see Appendix A) by assuming α fixed at its fault clearing value, and E' varying linearly with θ.

A drawback of both terminal voltage formulation and the E' formulation is that the resulting energy function expressions are lengthy and complicated. In both formulations, either the integration must be done with respect to some angle different from rotor angle θ (namely, β or γ), or some form of relation between θ and these angles must be assumed. These problems will be avoided in the next formulation which has been extensively tested on some test networks.

Constant E'_q and E'_d Formulation

From the discussions in the previous section and Chapter I, the following conclusions can be drawn:

> The classical model by assuming constant flux, does not entirely neglect the effect of exciter, rather it corresponds to a relatively weak excitation system. Thus, while the demagnetizing effects tend to reduce the machine flux, the exciter tends to boost the flux level. Therefore, a constant flux can be viewed as if an exciter is in operation.
>
> A modern high initial response excitation system rapidly increases the field winding flux during the first swing period.
>
> The effect of the flux increase can be approximately modeled by an average value which is held constant.

These concepts are schematically depicted in Figure 4.6, where point (a) corresponds to prefault values, point (b) is determined from the

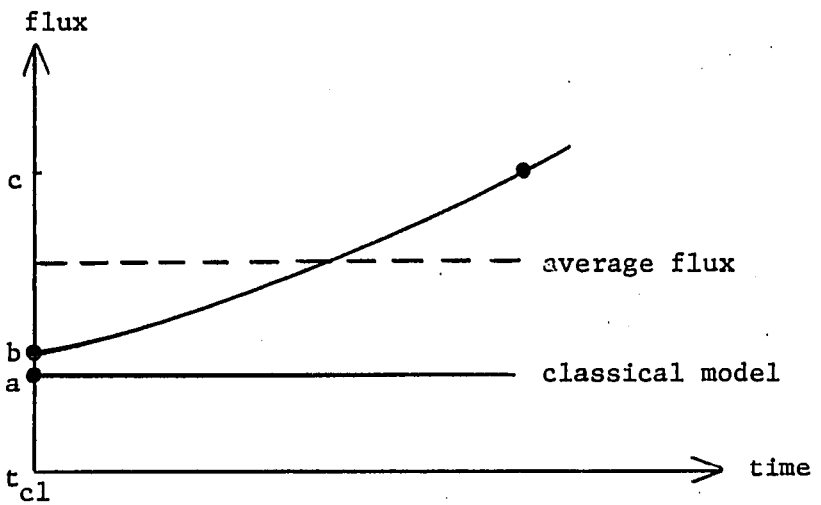

Figure 4.6. Typical variation of flux in the first swing

conditions at the end of the disturbance (e.g., at fault clearing), and point (c) is determined from the conditions at the UEP. Further discussion of this point is given in the next subsection. It is to be emphasized, however, that while a constant value of the internal generator voltage is used, the generator model used is not the classical model. The average flux in Figure 4.6 represents an approximation to the variation of flux for a two-axis model of generator.

The transient energy function

The transient energy function technique applied to the classical model of the power system exploits a very important characteristic of the system and the controlling UEP. Namely, a critically unstable trajectory passes "near" the controlling UEP, and this occurs when the potential energy assumes its maximum value, the kinetic energy becomes a minimum and nearly zero [21]. Based on these facts, it is stated that the controlling UEP determines the critical energy of the system.

It is claimed here that the same phenomenon holds true in the case of detailed representation and presence of exciter. The effect of exciter is merely to change the shape of the potential energy surfacing surrounding the region of stability (in the literature, this is called the potential energy boundary surface, PEBS). As mentioned earlier, the energy function is formulated as the first integral of the balance of power equation. Thus, if this integral is evaluated exactly, i.e., if the energy is computed along the actual solution trajectory by

numerical integration, then the total energy will remain constant for the postdisturbance period. By simulation, it appears that the critical trajectory actually passes near the controlling UEP, and it does so when the potential energy (computed along the solution trajectory) is at its maximum and the kinetic energy is minimum and its value is small. Therefore, it is assumed that the conditions at the controlling UEP determine the critical energy of a system represented in detail with exciter present.

Thus, the flux changes smoothly between the instant of removing the final disturbance and the UEP. An average, but constant, value of flux can adequately represent the variation of the flux. Since the d- and q-components of the generator flux are closely related to the internal voltages E'_q and E'_d, it will be assumed that E'_q and E'_d remain constant at a value given by

$$E'_q = \frac{1}{2}\left(E'^{UEP}_q + E'^{cl}_q\right), \quad E'_d = \frac{1}{2}\left(E'^{UEP}_d + E'^{cl}_d\right),$$

where the superscript cl indicates the instant of removing the final disturbance

Again, it is to be noted that the above model is not equivalent to the classical model; rather, it is an approximation to the two-axis model.

In the light of the above arguments, the assumption of constant E'_q and E'_d provides a reasonable way of incorporating the variation of flux due to exciter. As it will be shown shortly, this will result in a simple energy function.

The right-hand side of equation 2.42 represents the accelerating power. The electrical power is then given by:

$$P_{ei} = E'_{di} I_{di} + E'_{qi} I_{qi}, \quad i = 1, 2, \ldots n \tag{4.7}$$

In (4.7), if i belongs to the set of generators represented by the classical model, then $E'_{di} = 0$ and $E'_{qi} = E_i$. By substituting for I_{di} and I_{qi} from (2.44) and (2.45) into equation (4.7), then the electrical power can be written as:

$$P_{ei} = \sum_{j=1}^{n} \alpha_{ij} F_{G+B}(\theta_{ij}) + \beta_{ij} F_{B-G}(\theta_{ij}) \tag{4.8}$$

where

$$\alpha_{ij} = E'_{di} E'_{dj} + E'_{qi} E'_{qj}, \quad \beta_{ij} = E'_{di} E'_{qj} - E'_{qi} E'_{dj}.$$

Now, using (2.52) and (2.53) in (4.8) results in:

$$P_{ei} = \alpha_{ii} G_{ii} + \sum_{\substack{j=1 \\ j \neq 1}}^{n} [B_{ij}(\alpha_{ij} \sin \theta_{ij} + \beta_{ij} \cos \theta_{ij}) + G_{ij}(\alpha_{ij} \cos \theta_{ij} - \beta_{ij} \sin \theta_{ij})] \tag{4.9}$$

Since E'_q and E'_d are assumed to be constants, α_{ij} and β_{ij} will be constants and the energy function can be easily derived (see Appendix A). The kinetic energy is given by:

$$V_{KE} = \sum_{i=1}^{n} \frac{1}{2} M_i \tilde{\omega}_i^2 \tag{4.10}$$

and the change in potential energy is given by

$$\Delta V_{PE} = \sum_{i=1}^{n} - P_{Mi}(\theta_i^u - \theta_i^{cl}) + \sum_{i=1}^{n} \alpha_{ii} G_{ii}(\theta_i^u - \theta_i^{cl})$$

$$+ \sum_{i=1}^{n-1} \sum_{j=i+1}^{n} B_{ij}\alpha_{ij}[- \cos \theta_{ij}^u + \cos \theta_{ij}^{cl}]$$

$$+ B_{ij}\beta_{ij}[\sin \theta_{ij}^u - \sin \theta_{ij}^{cl}]$$

$$+ \sum_{i=1}^{n-1} \sum_{j=i+1}^{n} G_{ij}\alpha_{ij} \frac{\theta_i^u + \theta_j^u - \theta_i^{cl} - \theta_j^{cl}}{\theta_{ij}^u - \theta_{ij}^{cl}} [\sin \theta_{ij}^u - \sin \theta_{ij}^{cl}]$$

$$+ \sum_{i=1}^{n-1} \sum_{j=i+1}^{n} G_{ij}\beta_{ij} \frac{\theta_i^u + \theta_j^u - \theta_i^{cl} - \theta_j^{cl}}{\theta_{ij}^u - \theta_{ij}^{cl}} [\cos \theta_{ij}^u - \cos \theta_{ij}^{cl}] \tag{4.11}$$

CHAPTER V. TEST NETWORKS AND TEST PROCEDURES

Test Networks

Simulation and validation studies were conducted on three test power networks: a 4-generator system, a 20-generator equivalent of the BC Hydro system, and a 17-generator equivalent of the network of the state of Iowa.

The 4-generator test system

This test system, shown in Figure 5.1, is a modified version of the 9-bus, 3-machine system known as the WSCC test system. A fourth generator is connected to the original network through a double-circuit, 120-mile, 161-kV transmission line. The generator parameters are shown in Table 5.1. The fault location investigated is:

- 3-phase fault at bus #10, cleared by opening one of the lines 8-10

This test system was used primarily for testing the computer programs developed in this project and for validating the new procedures.

The 20-generator test system

This test system, shown in Figure 5.2, is a 50-bus, 20-generator equivalent of the power network of the BC Hydro system. The generator parameters are given in Table 5.1. The faults investigated are shown below:

- 3-phase fault at WSN500, cleared by removing line WSN500-KLY500
- 3-phase fault at KLY500, cleared by removing line KLY500-ING500

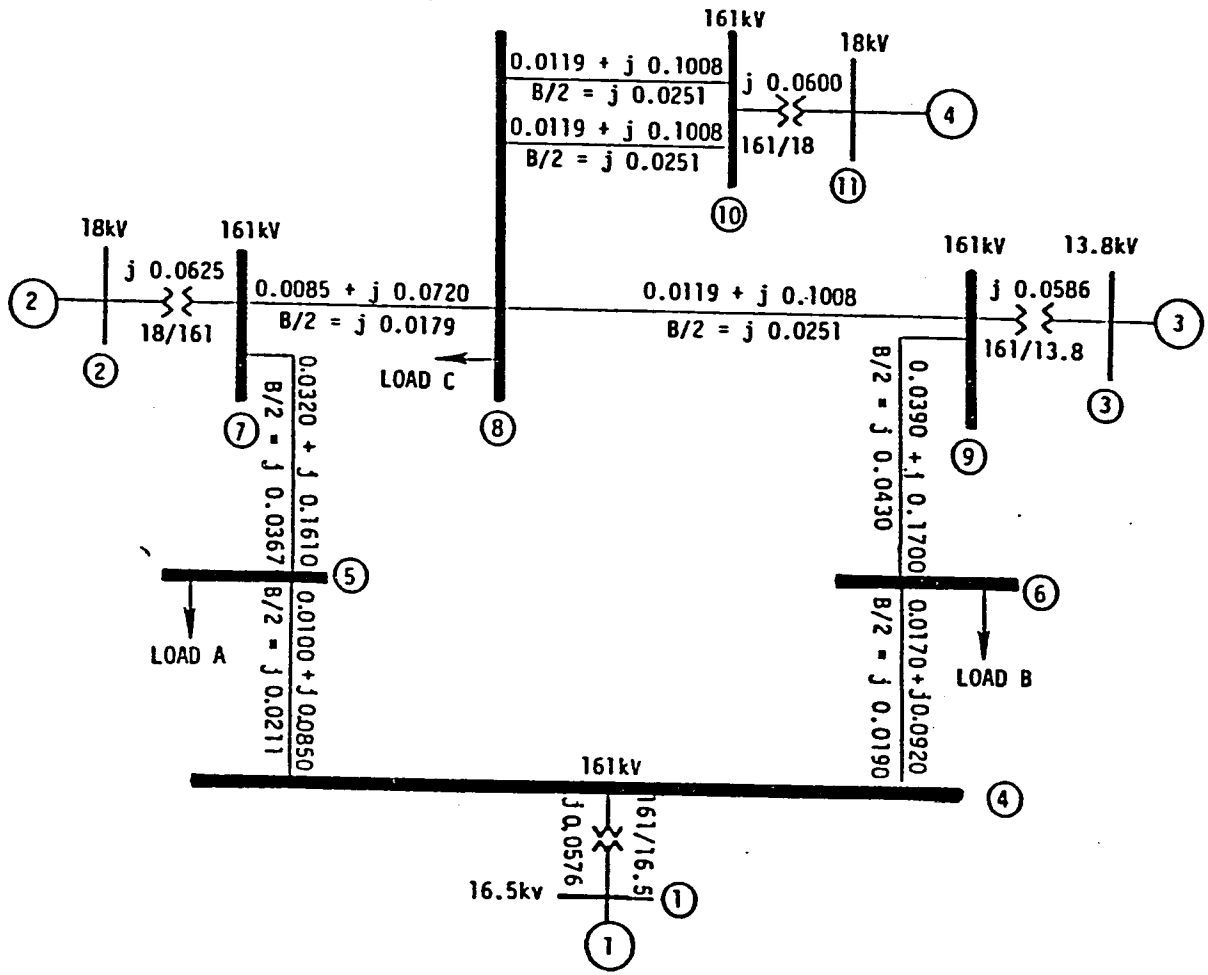

Figure 5.1. 4-generator test power system

Table 5.1. Generator data

No.	Gen. Name	H(sec)	x'_d	x'_q
(a) 4-generator system				
1	GEN 1	23.64	0.0608	
2	GEN 2	6.40	0.1198	0.1198
3	GEN 3	3.01	0.1813	
4	GEN11	6.40	0.1198	0.1198
(b) 20-generator (BC Hydro) system				
1	CHEAKMUS	6.42	0.1950	
2	BUNTZEN	3.17	0.3596	
3	BRIDGE1	6.56	0.1700	
4	BRIDGE2	9.47	0.1241	
5	RUSKIN	6.80	0.2765	
6	JOHNHART	4.28	0.2427	
7	STRATH-1	1.02	0.9600	
8	JORDAN R	6.33	0.1796	
9	GMS 6-8	117.28	0.0075	0.0075
10	P CANYON	28.78	0.3670	0.0367
11	MICA 1-4	100.54	0.0100	
12	SEVEN MI	22.34	0.0370	
13	K CANAL	28.40	0.0374	
14	BOUNDARY	116.20	0.0103	
15	CUSTER W	9999.99	0.0046	
16	WANETA A	8.33	0.1734	
17	WANETA B	7.96	0.1667	
18	BRILIANT	3.25	0.2867	
19	SSLOCANA	4.17	0.1721	
20	COLMAN	8.94	0.0967	

x_d	x_q	τ'_{d0}	τ'_{qo}	x_ℓ
0.8958	0.8645	6.00	0.54	0.0521
0.8958	0.8645	6.00	0.54	0.0521
0.0466	0.0222	4.90	0.06	0.0051
0.1005	0.0611	4.73	1.74	0.0272

Table 5.1. continued

No.	Gen. name	H(sec)	x'_d	x'_q
(c) 17-generator system (modified Iowa system)				
1	STJ0712	100.00	0.0040	
2	COOPR1G	34.56	0.0437	0.0437
3	FTRAD 4	80.00	0.0100	
4	WILMRT3	80.00	0.0050	
5	NEAL12G	16.79	0.0541	0.0541
6	NEAL34G	32.49	0.0197	0.0197
7	PRARK4G	6.65	0.1131	
8	MTOW 3G	2.66	0.3115	
9	AROL 1G	29.60	0.0535	
10	C.BL12G	5.00	0.1659	
11	DPS 57G	11.31	0.1148	
12	C.BL 3G	19.79	0.0297	
13	DVNPT 3	200.00	0.0020	
14	PALM710	200.00	0.0020	
15	PR ILD3	100.00	0.0040	
16	FT.CL1G	28.60	0.0559	
17	NEBCY1G	20.66	0.0544	

x_d	x_q	τ'_{d0}	τ'_{q0}	x_ℓ
0.1807	0.1755	6.54	1.08	0.0220
0.3570	0.3409	4.43	0.74	0.0298
0.1407	0.1354	4.00	0.67	0.0112

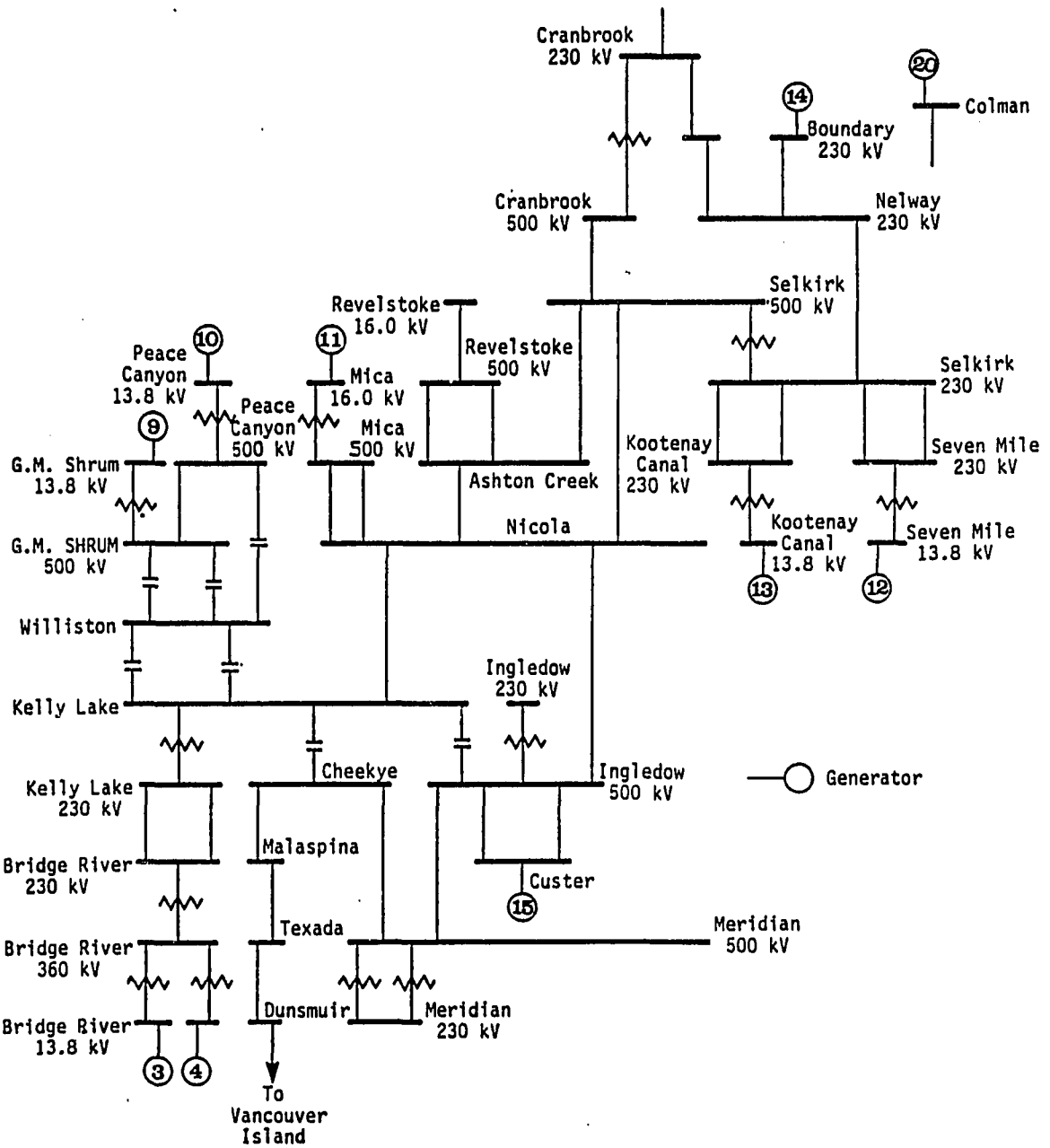

Figure 5.2. 20-generator system, BC Hydro's major transmission network

- 3-phase fault at GMS500, cleared by removing line GMS500-WSN500

This system was primarily used for validation of the transient energy function method developed in this project using a variety of disturbances at major high voltage buses, and determining the power transfer limit at a large generating station. This system is stability limited due to the long transmission distances to the main load center. The dynamic behavior of generators 3 (BRIDGE 1), 4 (BRIDGE 2), and particularly generators 9 (GMS) and 10 (P-CANYON) are of interest.

For the fault locations studied, the mode of disturbance remains the same as those of the system represented by the classical model.

17-generator (Modified Iowa System)

This is a 163-bus, 17-generator equivalent obtained from the base case set of data and the results of the NEAL 4 stability study [21]. A one-line diagram of the key buses of the system is given in Figure 5.3 and the generator data are given in Table 5.1. The following faults are investigated:

- 3-phase fault at RAUN, cleared by opening the line RAUN-LAKEFIELD
- 3-phase fault at COOPER, cleared by opening the line COOPER-BOONEVILLE

The area of interest in this network is the western part where several generating plants (on the Missouri River) are located. These generators are electrically close to each other, and a disturbance in that part of the network substantially influences the motion of several

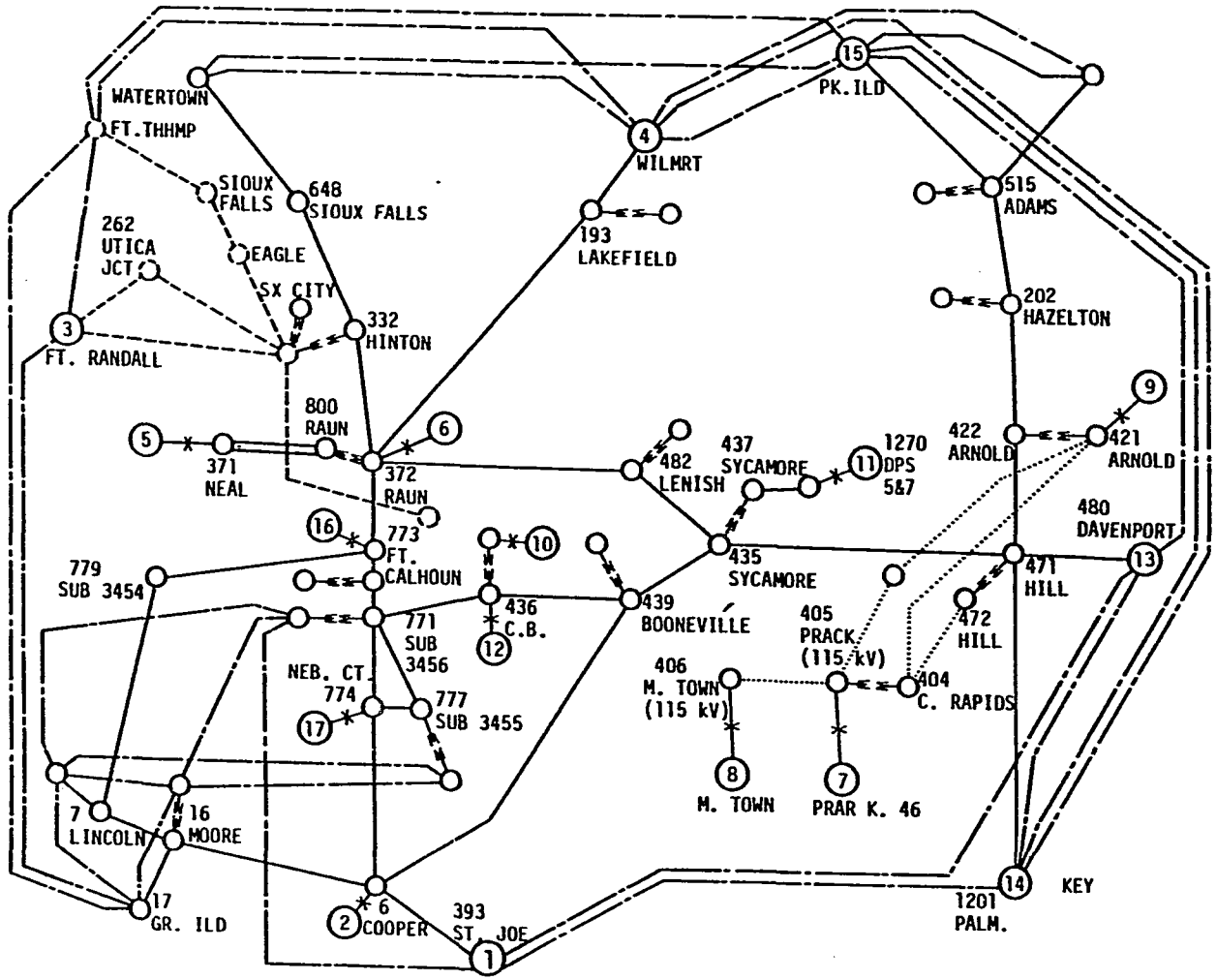

Figure 5.3. 17-generator system (Modified Iowa System)

generators. Thus, the modes of disturbance may be very complex. For the fault locations studied in this project, the exciter changed the mode of disturbance from that of the classical model.

Parameters of the Exciter

For the type G exciter shown in Figure 2.2, the following parameters were used.

Table 5.2. Parameters of type G exciter

Exciter #	Gain K	E_{FDmax}	E_{FDmin}	τ_E(sec)	K_F	τ_F
1	145	8.85	-8.85	0.05	0.	0.
2	135	7.50	-7.50	0.05	0.	0.
3	100	5.00	-5.00	0.05	0.	0.
4	45	4.00	-4.00	0.10	0.	0.

The parameters for exciters #1 and #2 are those of the BBC SCRX exciter on GMS and P-CANYON units of the BC Hydro system. The parameters for exciters #3 and #4 were chosen arbitrarily to reduce the effect of fast exciter for the purpose of testing and validation.

Test Procedure

Simple disturbance

Three phase faults at the specified locations in the three test networks are investigated. Critical clearing times for each fault is obtained by time solution using the EPRI Transient Mid-Term stability

program (Project RP-745). The proposed Transient Energy Function (TEF) method is then used for stability assessment and comparison is made to the time solution results.

One of the objectives of this study was to test the effect of excitation representation under the conditions of i) short fault duration, and ii) long fault duration. The 4-generator system and 17-generator system inherently exhibit longer critical clearing times than the 20-generator system.

Power transfer limit Although for the purposes of stability study the fault duration can be changed at will, in practice the duration of a fault is fixed by the time required for the protective devices to isolate the fault. Stability limits are often expressed as the power generation limit at a key station, or as the power transfer limit across a major transmission line. Motivated by this practice in industry, the 20-generator system was studied for a fault at WSN500 with fixed fault clearing time of 4 cycles [see reference 35]. For this fault, the maximum transient stability-limited generation level at GMS station (generator 9) is to be determined.

Complex disturbance

In the research reported upon in [35 and 36], the following sequence of disturbances were applied to the 20-generator system modeled classically.

1) Apply a 3-phase fault at WSN500 at $t = 0^+$.

2) At t = 4 cycles

   (i) Clear the fault by tripping circuit #1 line WSN500-KLY500

   (ii) Insert 100 MW of breaking resistor[1] at bus GMS138

3) At t = 9 cycles, the amount of generation needed to maintain stability is shed

4) At t = 35 cycles, the fault at WSN500 is applied by reclosing the tripped line

5) At t = 39 cycles, the fault cleared by tripping WSN500-KLY500

6) At t = 44 cycles, the 100 MW breaking resistor is disconnected.

The objective of the study was to determine, for a given generation level at GMS and P-CANYON stations, how much generation is to be shed from the GMS station at 9 cycles such that the system withstands the above sequence of disturbances before instability occurs.

The objective here is to determine the amount of generation shedding required when some of the generators are equipped with fast exciter.

Validation Results

Unstable equilibrium points

To validate the claim that the critically stable trajectory passes near UEP, the following test was conducted:

---

[1] A 400-MW breaking resistor is used in the research reported upon in [35 and 36]. However, 100 MW is used here in order to make the system unstable when 0. MW is shed at 9 cycles.

1) For a given disturbance scenario, the critically stable time solution was obtained

2) The change in potential energy was computed by integrating the postdisturbance accelerating powers with respect to the angles θ (in the COI frame) along the solution. Thus, the potential energy maximum was obtained.

3) For the given postdisturbance system, the unstable equilibrium points, as outlined in Chapter III, were obtained. This UEP was then compared to the value of the state variables at the instant of the potential energy maximum.

4-generator system The fault location investigated was bus 10 with one of the lines 8-10 removed to clear the fault. Generators 2 and 4 were represented by the two-axis model and equipped with the exciter 1 of Table 5.2. The critically stable trajectory was obtained by clearing the fault after 0.154 seconds. The UEP and the point on the solution trajectory corresponding to the maximum of the potential energy are given in Table 5.3.

20-generator system Generators 9 (GMS) and 10 (P-CANYON) were represented by the two-axis model; these generators were equipped with exciters 1 and 2 of Table 5.2, respectively. Critically stable trajectories were obtained for the following fault conditions:

i) Fault at WSN500 cleared after 6.4 cycles,

ii) Fault at KLY500 cleared after 7.2 cycles, and

iii) Fault at GMS500 cleared after 7.5 cycles

The UEP and the peak point of the trajectory for these faults are given in Tables 5.4-5.6.

Table 5.3. 4-generator system, 0.154 second fault at bus 10

State var.	Gen. #	UEP	Trajectory point
E'_q	2	1.340	1.319
E'_q	4	1.497	1.478
E'_d	2	-0.279	-0.298
E'_d	4	-0.217	-0.260
E_{FD}	2	4.102	3.970
E_{FD}	4	5.339	7.690
θ	1	-31.91	-30.11227
θ	2	- 5.91	- 9.15163
θ	3	-18.12	-18.09065
θ	4	132.30	128.88670

Table 5.4. 20-generator system, 6.4 cycle fault at WSN500

State var.	Gen. #	UEP	Trajectory point
E'_q	9	1.189	1.176
E'_q	10	1.318	1.327
E'_d	9	-0.200	-0.190
E'_d	10	-0.110	-0.144
E_{FD}	9	2.289	2.310
E_{FD}	10	1.895	3.690
θ	1	37.98	35.60
θ	2	17.47	16.05
θ	3	77.23	69.98
θ	4	71.49	66.27
θ	5	14.75	16.18
θ	6	23.49	21.22
θ	7	40.27	38.65
θ	8	40.08	43.73
θ	9	133.04	123.80
θ	10	131.63	134.98
θ	11	23.58	25.87
θ	12	42.88	43.54
θ	13	48.40	48.91
θ	14	42.80	43.23
θ	15	-3.24	-3.16
θ	16	42.57	42.70
θ	17	44.05	44.17
θ	18	43.85	44.33
θ	19	51.36	51.36
θ	20	29.10	29.99

Table 5.5. 20-generator system, 7.2 cycle fault at KLY500

State var.	Gen. #	UEP	Trajectory point
E'_q	9	1.183	1.127
E'_q	10	1.305	1.158
E'_d	9	-0.201	-0.206
E'_d	10	-0.112	-0.145
E'_{FD}	9	2.233	2.190
E'_{FD}	10	1.855	4.270
θ	1	64.02	48.65
θ	2	24.70	22.84
θ	3	125.60	96.53
θ	4	112.47	89.77
θ	5	21.23	18.84
θ	6	46.51	34.67
θ	7	67.25	61.22
θ	8	66.79	54.05
θ	9	133.65	120.33
θ	10	132.26	132.56
θ	11	33.73	34.56
θ	12	55.87	56.36
θ	13	61.47	60.72
θ	14	55.93	55.43
θ	15	-3.73	-3.51
θ	16	55.67	54.96
θ	17	57.18	56.46
θ	18	57.00	57.18
θ	19	64.65	64.06
θ	20	41.70	42.48

Table 5.6. 20-generator system, 7.5 cycle fault at GMS500

State var.	Gen. #	UEP	Trajectory point
E'_q	9	1.254	1.218
E'_q	10	1.432	1.380
E'_d	9	-0.179	-0.201
E'_d	10	-0.098	-0.138
E_{FD}	9	2.638	2.100
E_{FD}	10	2.193	3.470
θ	1	51.91	54.49
θ	2	23.90	22.74
θ	3	107.92	106.50
θ	4	94.05	97.63
θ	5	20.93	27.57
θ	6	34.90	32.26
θ	7	54.31	55.25
θ	8	57.56	64.02
θ	9	140.42	123.74
θ	10	138.55	131.83
θ	11	31.78	32.40
θ	12	53.67	46.75
θ	13	59.25	51.93
θ	14	53.71	46.06
θ	15	-3.72	-3.37
θ	16	53.43	45.36
θ	17	54.94	46.83
θ	18	54.76	47.18
θ	19	62.39	55.06
θ	20	39.49	32.35

Energy function

The (constant E'_q and E'_d formulation) energy function of Chapter IV was tested against the time solution results to determine its validity. The test procedure is as follows:

i) The exact change in potential energy was computed along the solution trajectory from

$$\Delta V_{PE|\text{trajectory}}(t) = \sum_{i=1}^{n} \int_{\theta_i^{cl}}^{\theta_i(t)} \tilde{P}_{\alpha i} d\theta_i$$

since $V_{PE}(t_{cl}) \triangleq 0$, ΔV_{PE} is computed with respect to the potential energy at clearing.

ii) The potential energy component of the proposed energy function (see equation (4.11)) was computed at various instants along the solution by replacing θ_i^u, E'^u_{qi}, E'^u_{di} with values of $\theta_i(t)$, $E'_{qi}(t)$, $E'_{di}(t)$.

The time solutions used for this study corresponded to critically stable cases. Since at the instant of the maximum of the potential energy, i.e., maximum of $\Delta V_{PE|\text{trajectory}}(t)$, the solution trajectory passes near the UEP, it is sufficient to compare the two potential energies up to that instant. The results of this comparison for the three test networks is given in Tables 5.7-5.12. We note from the data in these tables that at the instant $\Delta V_{PE|\text{trajectory}}$ is at its peak value, the values of ΔV_{PE} in both columns are of similar magnitudes.

Table 5.7. 4-generator system. Potential energy comparison. Fault at bus 10, cleared in 0.154 second

Time	$\Delta\ddot{V}_{PE}\|_{trajectory}(t)$	$\Delta V_{PE}(t)$
0.1540	0.0000	0.0000
0.1940	0.0804	0.0804
0.2340	0.1838	0.1814
0.2740	0.2950	0.2877
0.3140	0.3988	0.3848
0.3540	0.4826	0.4617
0.3940	0.5404	0.5130
0.4340	0.5738	0.5409
0.4740	0.5898	0.5527
0.5140	0.5969	0.5579
0.5540	0.6013	0.5639
0.5940	0.6054	0.5748
0.6340	0.6085	0.5909
0.6740	0.6095	0.6117
0.7140	0.6090	0.6377
0.7540	0.6092	0.6702
0.7940	0.6114	0.7098
0.8340	0.6144	0.7503
0.8740	0.6143	0.7795
0.9140	0.6056	0.7923
0.9540	0.5815	0.7887
0.9940	0.5321	0.7682

Table 5.8. 20-generator system. Potential energy comparison. Fault at bus WSN500, cleared in 6.4 cycles

Time	$\Delta V_{PE\|trajectory}(t)$	$\Delta V_{PE}(t)$
0.1067	0.0000	0.0000
0.1567	0.5588	0.5188
0.2067	1.2934	1.0216
0.2567	1.8067	1.3900
0.3067	2.1240	1.8747
0.3567	2.4068	2.5498
0.4067	2.7901	3.3189
0.4567	3.2795	4.0355
0.5067	3.7150	4.5467
0.5567	3.9210	4.7514
0.6067	3.8961	4.6880
0.6567	3.8212	4.5357
0.7067	3.8794	4.4882
0.7567	4.0787	4.6131
0.8067	4.2585	4.8107
0.8567	4.2603	4.9437
0.9067	4.0980	4.9855
0.9567	3.9633	5.0518
1.0067	4.0239	5.2598

Figure 5.9. 20-generator system. Potential energy comparison. Fault at bus KLY500, cleared in 7.2 cycles

Time	$\Delta V_{PE\|trajectory}(t)$	$\Delta V_{PE}(t)$
0.1200	0.0000	0.0000
0.1700	1.0355	0.9888
0.2200	2.1188	1.8044
0.2700	2.8078	2.3702
0.3200	3.2082	3.0211
0.3700	3.5540	3.8511
0.4200	4.0145	4.7542
0.4700	4.5677	5.5557
0.5200	5.0057	6.0758
0.5700	5.1597	6.2298
0.6200	5.0907	6.1159
0.6700	5.0316	5.9733
0.7200	5.1523	5.9949
0.7700	5.3975	6.1954
0.8200	5.5524	6.4180
0.8700	5.4583	6.5054
0.9200	5.1826	6.4684
0.9700	4.9693	6.4756
1.0200	4.9681	6.6246

Table 5.10. 20-generator system. Potential energy comparison. Fault at bus GMS500, cleared in 7.5 cycles

Time	$\Delta V_{PE\|trajectory}(t)$	$\Delta V_{PE}(t)$
0.1250	0.0000	0.0000
0.1750	1.4027	1.3605
0.2250	3.0165	2.7315
0.2750	4.2852	3.7391
0.3250	5.1250	4.5667
0.3750	5.7060	5.3813
0.4250	6.2116	6.1767
0.4750	6.6848	6.8438
0.5250	7.0075	7.2436
0.5750	7.0720	7.3173
0.6250	6.9444	7.1547
0.6750	6.8181	6.9557
0.7250	6.8195	6.8783
0.7750	6.8791	6.9327
0.8250	6.8122	6.9997
0.8750	6.4928	6.9649
0.9250	5.9850	6.8367

Table 5.11. 17-generator system. Potential energy comparison. Fault at bus RAUN, cleared in 0.179 seconds

Time	$\Delta V_{PE\|trajectory}(t)$	$\Delta V_{PE}(t)$
0.1790	0.0000	0.0000
0.2290	3.6989	3.7698
0.2790	5.7754	5.9019
0.3290	6.5914	6.8872
0.3790	6.7249	7.8889
0.4290	6.5530	7.8284
0.4790	6.2396	8.4008

Table 5.12. 17-generator system. Potential energy comparison. Fault at bus COOPER, cleared in 0.219 seconds

Time	$\Delta V_{PE\|trajectory}(t)$	$\Delta V_{PE}(t)$
0.2190	0.0000	0.0000
0.2690	4.5866	4.6679
0.3190	7.2392	7.3780
0.3690	8.4032	8.6199
0.4190	8.8126	9.1275
0.4690	8.9996	9.4177
0.5190	9.2234	9.7346
0.5690	9.5389	10.1247
0.6190	9.8957	10.5366
0.6690	10.1999	10.8828
0.7190	10.2996	11.0325
0.7690	9.9251	10.7532
0.8190	8.6456	9.6841
0.8690	5.7977	7.2878

CHAPTER VI. TRANSIENT STABILITY ASSESSMENT RESULTS

Procedure for Transient Stability Assessment

The procedure for transient stability assessment using the transient energy function with the effect of exciter included is outlined below.

Step 1: Determine the postdisturbance admittance matrix reduced to the internal nodes of the generator. The transient reactance, x'_d, is included in the admittance matrix for all of the generators.

Step 2: Determine the predisturbance value of the state variables E'_{qi}, E'_{di}, E_{FDi}, θ_i, $\tilde{\omega}_i$.

Step 3: Assuming the Mode of Disturbance (MOD) is known, advance the angles of the MOD group beyond 90 degrees by computing $\pi-\theta^s_m$, where θ^s_m are the predisturbance values of the MOD group. Use the predisturbance values of the rest of the variables along with the angles advanced as the starting values for the UEP solution. If necessary, correct for motion of center of inertia.

Step 4: Compute E'_q, E'_d, θ, and $\tilde{\omega}$ for all machines at the end of the disturbance.

Step 5: For the given MOD, make a correction to the kinetic energy [19,21] to remove the energy that does not contribute to the system separation. $V_{KE_{corrected}} = \frac{1}{2} M_{eq} \tilde{\omega}^2_{eq}$ where, $M_{eq} = M_{cr}M_{sys}/(M_{cr} + M_{sys})$, $\tilde{\omega}_{eq} = (\tilde{\omega}_{cr} - \tilde{\omega}_{sys})$ in which M_{cr}, $\tilde{\omega}_{cr}$, M_{sys}, and $\tilde{\omega}_{sys}$ designate the center of inertia and the speed of the critical group, and the rest of the system, respectively.

Step 6: Using $E'_q = \frac{1}{2}(E'^{u}_q + E'^{cl}_q)$, $E'_d = \frac{1}{2}(E'^{u}_d + E'^{cl}_d)$

Compute $\Delta V_{PE} = V_{PE}\Big|^{UEP}_{clearing}$

Step 7: Compute the energy margin from $\Delta V = \Delta V_{PE} - V_{KE}|_{corrected}$. The system is unstable if $\Delta V < 0$, otherwise it is stable.

Test Results

Simple disturbance

The proposed transient energy function (TEF) technique was applied to make stability assessment for the three phase faults described in Chapter V.

4-generator system Generators 2 and 4 were represented by the two-axis model and equipped with exciter 1 of Table 5.2. The fault was cleared after 0.154 seconds. Table 6.1 shows that TEF technique and time solution make similar stability assessments.

Table 6.1. Stability assessment[a] for the fault at bus 10 of the 4-generator system. $t_{cl} = 0.154$ sec

V_{KE} corrected for generator	$V_{KE}\|_{corrected}$	$V_{PE}\|^{UEP}_{cl}$	$V\|^{UEP}_{cl}$	TEF assessment	Critical clearing time (sec)
4	0.6164	0.7048	0.0884	Stable	$0.154<t_{cr}<0.156$

[a]The UEPs are given in Table 5.3.

20-generator system Generators 9 and 10 were represented by the two-axis model and equipped with exciters 1 and 2 of Table 5.2, respectively. The results are displayed in Tables 6.2-6.4.

Table 6.2. Stability assessment[a] for the fault at bus WSN500 of the 20-generator system. t_{cl} = 6.4 cycles

V_{KE} corrected for generator	$V_{KE}\|_{corrected}$	$V_{PE}\|^{UEP}_{cl}$	$V\|^{UEP}_{cl}$	TEF assessment	Critical clearing time (cycles)
9,10	4.4201	4.8196	0.3995	Stable	$6.4<t_{cr}<6.6$

[a]The UEPs are given in Table 5.4.

Table 6.3. Stability[a] for the fault at bus KLY500 of the 20-generator system. t_{cl} = 7.2 cycles

V_{KE} corrected for generator	$V_{KE}\|_{corrected}$	$V_{PE}\|^{UEP}_{cl}$	$V\|^{UEP}_{cl}$	TEF assessment	Critical clearing time (cycles)
3,4,9,10	5.6392	6.3697	0.7305	Stable	$7.2<t_{cr}<7.4$

[a]The UEPs are given in Table 5.5.

Table 6.4. Stability assessment[a] for the fault at bus GMS500 of the 20-generator system. t_{cr} = 7.5 cycles

V_{KE} corrected for generator	$V_{KE}\|_{corrected}$	$V_{PE}\|^{UEP}_{cl}$	$V\|^{UEP}_{cl}$	TEF assessment	Critical clearing time (cycles)
3,4,9,10	7.6630	6.8754	-0.7576	Unstable	$7.5<t_{cr}<7.8$

[a]The UEPS are given in Table 5.6.

Table 6.4 shows that for the fault at GMS500, TEF method predicts a critical clearing time of slightly less than 7.5 cycles.

17-generator system For the fault at RAUN, the generators 5 and 6 were represented by the two-axis model and equipped with the exciter 1 of Table 5.2. For this case, the minimization algorithm failed to converge to a UEP. Closer examination of the time solution results indicated that the mode of disturbance is rather complex. Figures 6.1 and 6.2 show that 8 generators tend to lose synchronism with the rest of the system. Studies reported upon in Reference [21] show that when all of the generators are modeled classically the mode of disturbance is that of 5 and 6 alone. The apparent change of the mode of disturbance is due to the presence of fast exciter.

Next, a slower exciter, exciter 4 of Table 5.2, was used on generators 5 and 6. Figures 6.3 and 6.4 show that only generators 5 and 6 lose synchronism with the system; however, generator 16 (FT. CAL) is severely disturbed. The only UEP solution obtained is given in Table 6.5. The UEP solution does not reflect the effect of disturbance on generator 16. Thus, it appears that the UEP solution of Table 6.5 is not the relevant UEP. As a result, the TEF for the given UEP predicts instability while the case under study is critically unstable as shown in Table 6.6.

For the fault at COOPER, generator 2 is represented by the two-axis model and equipped with exciter 1 of Table 5.2. In the UEP solution, the minimization algorithm did not terminate normally. However,

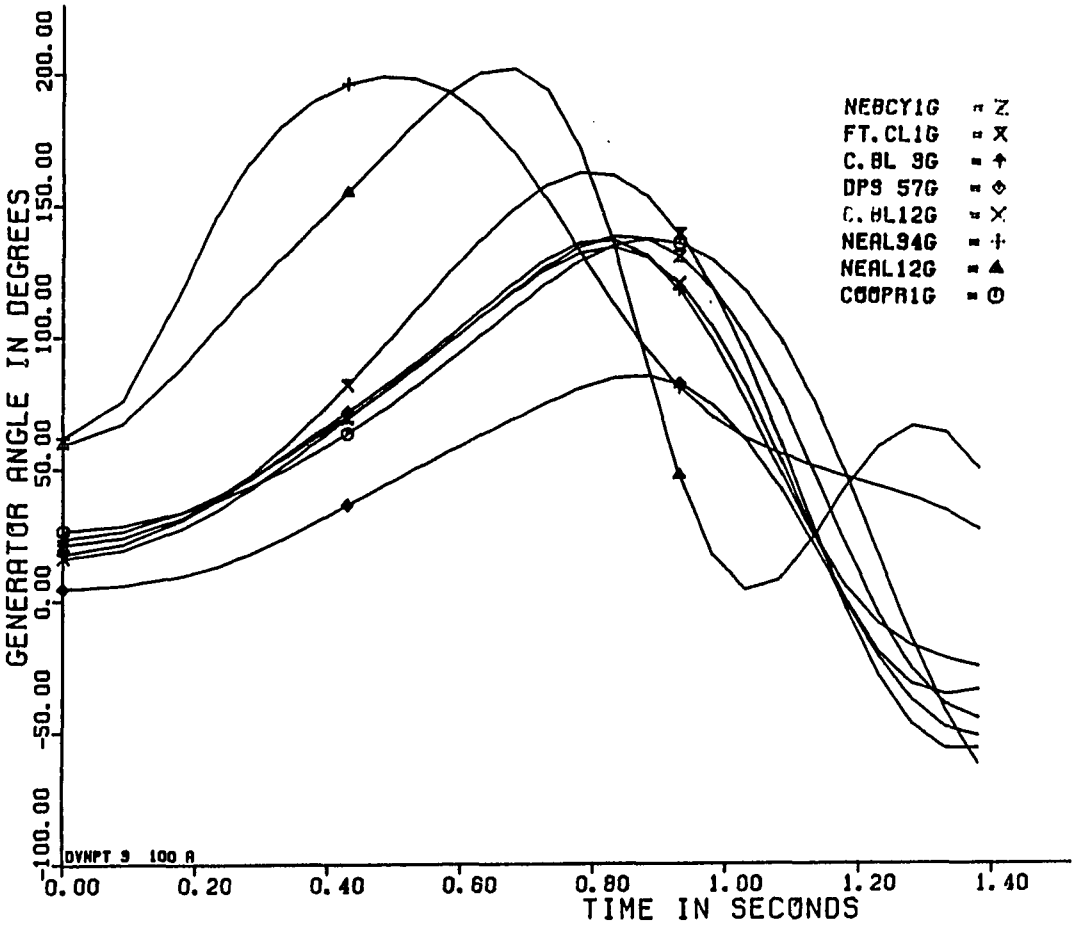

Figure 6.1. 17-generator system. Fault at RAUN cleared in 0.179 sec. Fast exciter case

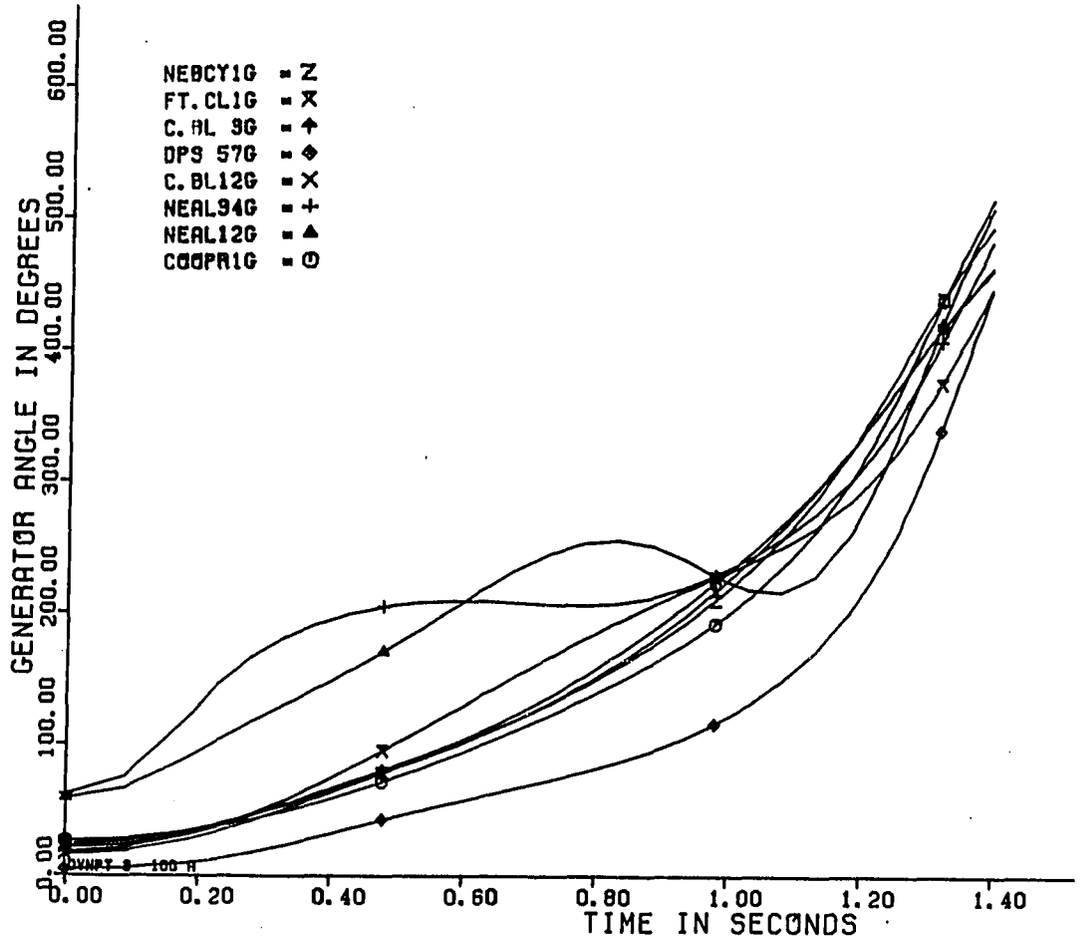

Figure 6.2. 17-generator system. Fault at RAUN cleared in 0.180 sec. Fast exciter case

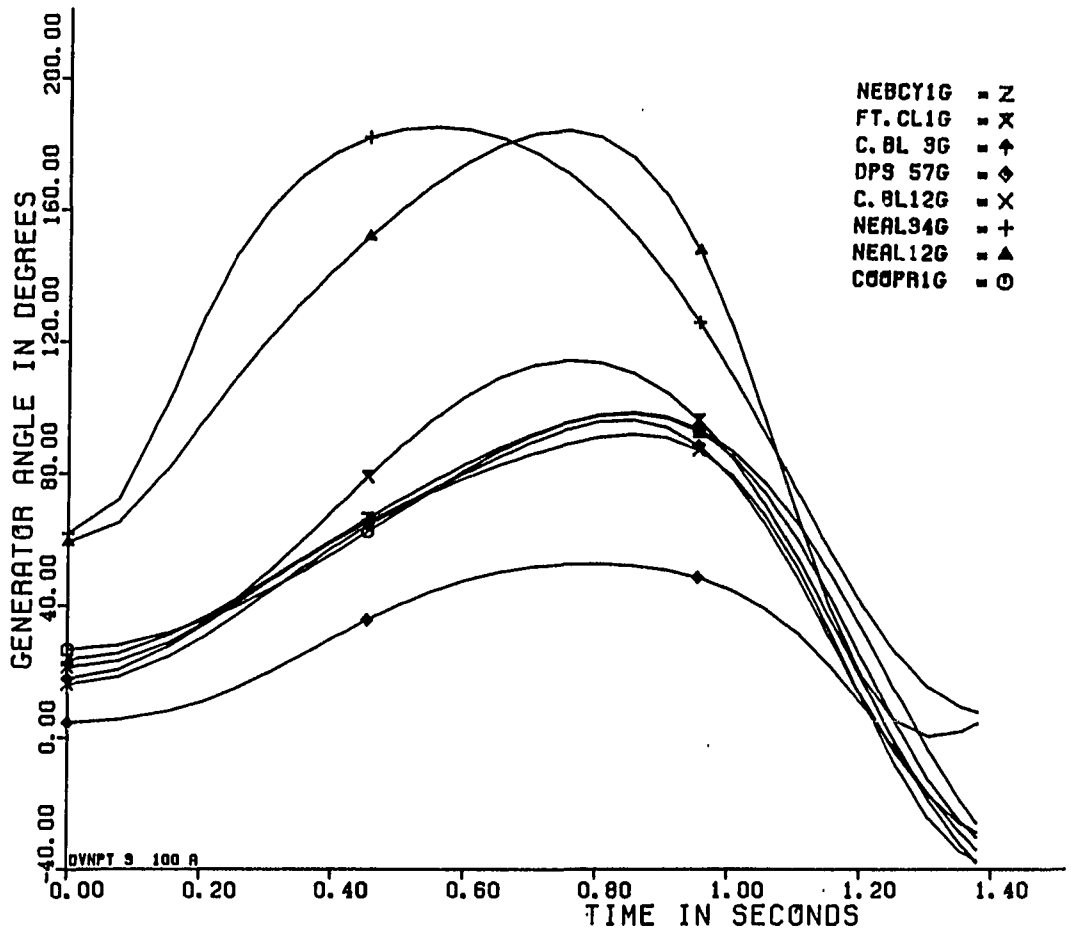

Figure 6.3. 17-generator system. Fault at RAUN cleared in 0.153 sec. Slow exciter case

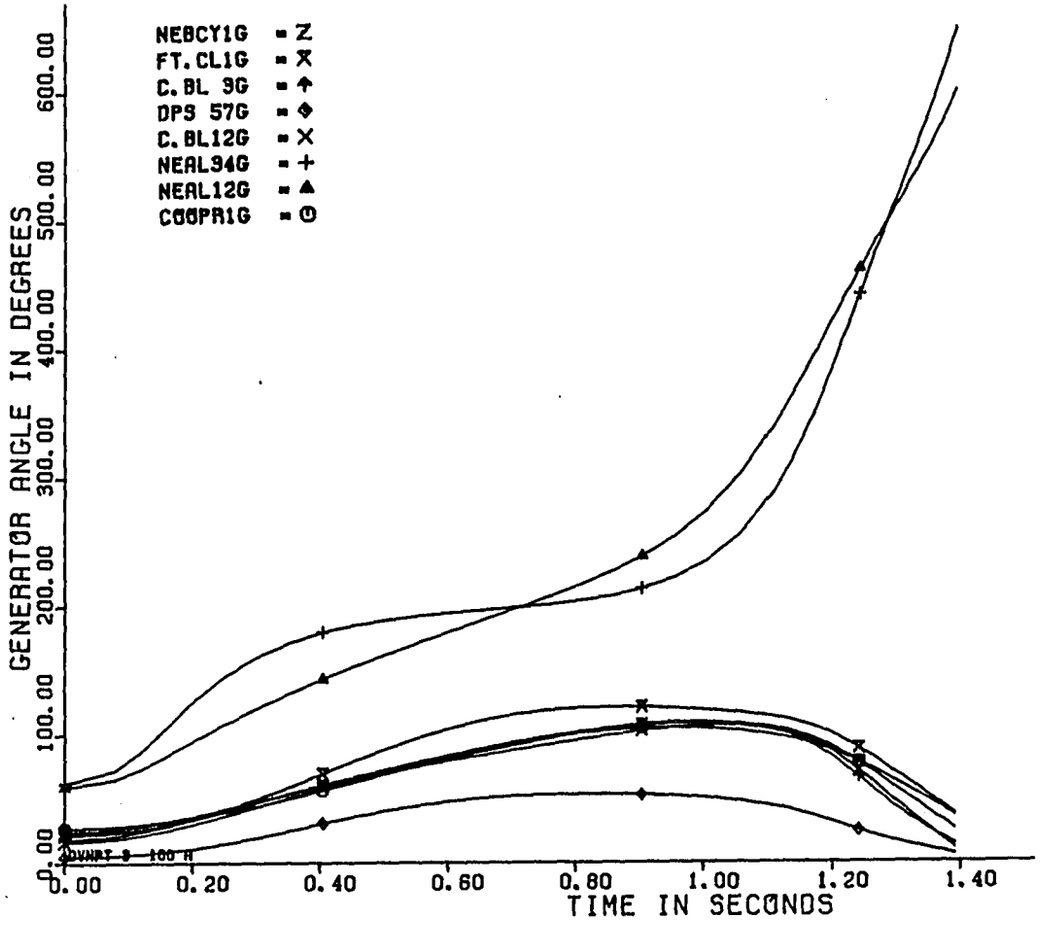

Figure 6.4. 17-generator system. Fault at RAUN cleared in 0.154 sec. Slow exciter case

Table 6.5. 17-generator system. Fault at RAUN slow exciter case

State var.	Gen. #	UEP
E'_q	5	0.805
E'_q	6	0.715
E'_d	5	-0.305
E'_d	6	-0.294
E_{FD}	5	4.000
E_{FD}	6	4.000
θ	1	-5.10
θ	2	35.84
θ	3	8.59
θ	4	-19.87
θ	5	137.75
θ	6	157.48
θ	7	-13.41
θ	8	-7.93
θ	9	-3.99
θ	10	37.27
θ	11	5.61
θ	12	34.83
θ	13	-22.36
θ	14	-20.71
θ	15	-13.74
θ	16	45.02
θ	17	37.18

Table 6.6. 17-generator system. Stability assessment for the fault at RAUN, cleared in 0.153 seconds

V_{KE} corrected for generator	$V_{KE}\|_{corrected}$	$V_{PE}\|^{UEP}_{cl}$	$V\|^{UEP}_{cl}$	TEF assessment	Critical clearing time (sec)
5,6	7.0367	3.5171	-3.5197	Unstable	$0.153<t_{cr}<0.154$

at a certain iteration the mismatch function was small. This point has been reported as the UEP solution in Table 6.7. The value of E'_q is unusually high, and the exciter voltage is at the limit. Obviously, this UEP solution is not the relevant UEP and it will result in erroneous stability assessment.

Power transfer limit

For this study on the 20-generator system, the fault clearing time is held fixed at 4 cycles. The test conditions are:

Fault: WSN500, cleared at 4 cycles
Line cleared: WSN500-KLY500
Generator 9: Exciter #1
Generator 10: Exciter #2

Time solution results show that, for this fault, the system is stable when generator 9 operates at 2334 MW at steady state conditions; and the system is critically stable at the generation level of 2374 MW. Increasing this generation level to 2384 MW causes instability for this fault. Tables 6.8 and 6.10 show the UEP solutions for the 2334 MW and 2374 MW cases. Stability assessment results are given in Tables 6.9 and 6.11.

Table 6.7. 17-generator system. Fault at COOPER

State var.	Gen. #	UEP
E'_q	2	2.482
E'_d	2	-0.188
E_{FD}	2	8.85
θ	1	-11.70
θ	2	179.86
θ	3	7.35
θ	4	-10.87
θ	5	30.77
θ	6	33.37
θ	7	-14.88
θ	8	-11.20
θ	9	-5.18
θ	10	44.08
θ	11	-0.05
θ	12	48.55
θ	13	-24.37
θ	14	-23.61
θ	15	-7.81
θ	16	46.77
θ	17	85.93

Table 6.8. 20-generator system. GMS generation at 2334 MW

State var.	Gen. #	UEP	State var.	Gen. #	UEP
E'_q	9	1.179	θ	8	41.65
E'_q	10	1.301	θ	9	128.75
E'_d	9	-0.214	θ	10	125.66
E'_d	10	-0.112	θ	11	22.26
E_{FD}	9	2.261	θ	12	40.88
E_{FD}	10	1.847	θ	13	46.39
θ	1	35.35	θ	14	40.77
θ	2	16.33	θ	15	-3.10
θ	3	70.20	θ	16	40.56
θ	4	65.02	θ	17	42.03
θ	5	13.70	θ	18	41.83
θ	6	21.50	θ	19	49.30
θ	7	37.81	θ	20	27.21

Table 6.9. Stability assessment for the 20-generator system. GMS generation at 2334 MW

V_{KE} corrected for generator	$V_{KE}\|_{corrected}$	$V_{PE}\|^{UEP}_{cl}$	$V\|^{UEP}_{cl}$	TEF assessment	Time solution assessment
9,10	1.9562	2.6663	0.7101	Unstable	Unstable

Table 6.10. 20-generator system. GMS generation at 2374 MW

State var.	Gen. #	UEP	State var.	Gen. #	UEP
E'_q	9	1.176	θ	8	40.99
E'_q	10	1.295	θ	9	127.49
E'_d	9	-0.219	θ	10	123.95
E'_d	10	-0.113	θ	11	21.89
E_{FD}	9	2.251	θ	12	40.32
E_{FD}	10	1.833	θ	13	45.82
θ	1	34.64	θ	14	40.20
θ	2	16.00	θ	15	-3.06
θ	3	68.46	θ	16	40.00
θ	4	63.41	θ	17	41.47
θ	5	13.40	θ	18	41.26
θ	6	20.95	θ	19	48.72
θ	7	37.13	θ	20	26.67

Table 6.11. Stability assessment for the 20-generator system. GMS generation at 2374 MW

V_{KE} corrected for generator	$V_{KE}\|_{corrected}$	$V_{PE}\|^{UEP}_{cl}$	$V\|^{UEP}_{cl}$	TEF assessment	Time solution assessment
9,10	2.0135	2.2342	0.2207	Stable	Stable

Complex disturbance

The complex disturbance outlined in Chapter V is applied to the 20-generator system for a fault at WSN500. The predisturbance generation level at generator 9 is 2457 MW. To simulate the generation shedding scheme when the TEF method is used, the postdisturbance reduced admittance matrix and the UEPs were computed assuming that the generation dropped is eventually picked up by other generators in proportion to their inertias. Since the 20-generator system has an equivalent generator with an infinite inertia, all the generation dropped is assigned to it.

Table 6.12 shows the UEPs for the base case (zero MW shed at 9 cycles), and Table 6.13 displays the stability assessment results. The results of the study for generation shedding of 270 MW (1 unit at the GMS station) are given in Tables 6.14 and 6.15. Next, different levels of generation shedding were studied and the results are reported in Tables 6.15-6.21. It must be noted that shedding a fraction of a unit (e.g., 196 MW or 147 MW) may not be physically meaningful, however, this is done only to compare the TEF method with the time solution method in the marginally stable or unstable cases.

Classical Model vs. Exciter Representation

The results of this section are based on time solution. The objective is to arrive at qualitative assessment regarding the range of applicability of the classical model.

Table 6.12. Complex disturbance study. No generation shed at 9 cycles

State var.	Gen. #	UEP	State var.	Gen. #	UEP
E'_q	9	1.167	θ	8	39.56
E'_q	10	1.282	θ	9	124.51
E'_d	9	-0.229	θ	10	120.01
E'_d	10	-0.115	θ	11	21.14
E_{FD}	9	2.225	θ	12	39.20
E_{FD}	10	1.798	θ	13	44.70
θ	1	33.14	θ	14	39.07
θ	2	15.30	θ	15	-2.98
θ	3	65.06	θ	16	38.88
θ	4	60.22	θ	17	40.35
θ	5	12.76	θ	18	40.13
θ	6	19.96	θ	19	47.56
θ	7	35.83	θ	20	25.61

Table 6.13. Stability assessment for complex disturbance study. No generation shed at 9 cycles

V_{KE} corrected for generator	$V_{KE}\|_{corrected}$	$V_{PE}\|^{UEP}_{cl}$	$V\|^{UEP}_{cl}$	TEF assessment	Time solution assessment
9,10	3.6998	0.0371	-3.6627	Unstable	Unstable

Table 6.14. Complex disturbance study. 270 MW shed at 9 cycles

State var.	Gen. #	UEP	State var.	Gen. #	UEP
E'_q	9	1.213	θ	8	42.74
E'_q	10	1.324	θ	9	134.86
E'_d	9	-0.213	θ	10	132.02
E'_d	10	-0.109	θ	11	22.86
E_{FD}	9	2.477	θ	12	41.88
E_{FD}	10	1.910	θ	13	47.40
θ	1	36.41	θ	14	41.79
θ	2	16.52	θ	15	-3.05
θ	3	74.21	θ	16	41.58
θ	4	68.53	θ	17	43.06
θ	5	13.92	θ	18	42.85
θ	6	22.25	θ	19	50.33
θ	7	39.09	θ	20	28.13

Table 6.15. Stability assessment for complex disturbance study. 270 MW shed at 9 cycles

V_{KE} corrected for generator	$V_{KE}\|_{corrected}$	$V_{PE}\|^{UEP}_{cl}$	$V\|^{UEP}_{cl}$	TEF assessment	Time solution assessment
9,10	0.1135	2.4980	2.3845	Stable	Stable

Table 6.16. Complex disturbance study. 196 MW shed at 9 cycles

State var.	Gen. #	UEP	State var.	Gen. #	UEP
E'_q	9	1.203	θ	8	41.96
E'_q	10	1.315	θ	9	132.35
E'_d	9	-0.215	θ	10	129.07
E'_d	10	-0.110	θ	11	22.46
E_{FD}	9	2.408	θ	12	41.23
E_{FD}	10	1.884	θ	13	46.75
θ	1	35.59	θ	14	41.13
θ	2	16.24	θ	15	-3.04
θ	3	71.68	θ	16	40.93
θ	4	66.25	θ	17	42.40
θ	5	13.66	θ	18	42.19
θ	6	21.71	θ	19	49.66
θ	7	38.30	θ	20	27.52

Table 6.17. Stability assessment for complex disturbance study. 196 MW shed at 9 cycles

V_{KE} corrected for generator	$V_{KE}\|_{corrected}$	$V_{PE}\|^{UEP}_{cl}$	$V\|^{UEP}_{cl}$	TEF assessment	Time solution assessment
9,10	0.4791	1.0593	0.5802	Stable	Stable

Table 6.18. Complex disturbance study. 172 MW shed at 9 cycles

State var.	Gen. #	UEP	State var.	Gen. #	UEP
E'_q	9	1.198	θ	8	41.69
E'_q	10	1.311	θ	9	131.51
E'_d	9	-0.217	θ	10	128.04
E'_d	10	-0.111	θ	11	22.31
E_{FD}	9	2.384	θ	12	41.00
E_{FD}	10	1.875	θ	13	46.52
θ	1	35.31	θ	14	40.90
θ	2	16.14	θ	15	-3.04
θ	3	70.84	θ	16	40.70
θ	4	65.50	θ	17	42.17
θ	5	13.56	θ	18	41.96
θ	6	21.52	θ	19	49.42
θ	7	38.02	θ	20	27.31

Table 6.19. Stability assessment for complex disturbance study. 172 MW shed at 9 cycles

V_{KE} corrected for generator	$V_{KE\|corrected}$	$V_{PE}\|^{UEP}_{cl}$	$V\|^{UEP}_{cl}$	TEF assessment	Time solution assessment
9,10	0.6778	0.6788	0.0011	Stable	Stable

Table 6.20. Complex disturbance study. 147 MW shed at 9 cycles

State var.	Gen. #	UEP	State var.	Gen. #	UEP
E'_q	9	1.194	θ	8	41.41
E'_q	10	1.308	θ	9	130.61
E'_d	9	-0.219	θ	10	127.00
E'_d	10	-0.111	θ	11	22.16
E_{FD}	9	2.363	θ	12	40.77
E_{FD}	10	1.866	θ	13	46.28
θ	1	35.02	θ	14	40.66
θ	2	16.04	θ	15	-3.03
θ	3	70.01	θ	16	40.46
θ	4	64.75	θ	17	41.94
θ	5	13.46	θ	18	41.73
θ	6	21.32	θ	19	49.18
θ	7	37.74	θ	20	27.10

Table 6.21. Stability assessment for complex disturbance study. 147 MW shed at 9 cycles

V_{KE} corrected for generator	$V_{KE}\|_{corrected}$	$V_{PE}\|^{UEP}_{cl}$	$V\|^{UEP}_{cl}$	TEF assessment	Time solution assessment
9,10	0.9241	0.3577	-0.5664	Unstable	Unstable

The results of tests on power transfer limit reported in the previous sections is compared to that of the system represented by the classical model in Tables 6.22a and 6.22b.

Table 6.22a. 4-cycle fault at WSN500 with Exciter #1 on generator 9 and Exciter #2 on generator 10

Generation level at generator 9	System condition
2374 MW	Stable
2384 MW	Unstable

Table 6.22b. 4-cycle fault at WSN500. All generators represented by the classical model

Generation level at generator 9	System condition
2030 MW	Stable
2040 MW	Unstable

Tables 6.22 show that for faults of short duration, indeed, the exciter increases the region of stability. However, for faults of longer duration, the classical model is similar to a very fast excitation system (Table 6.23).

Table 6.23. 17-generator system. Fault at RAUN. Critical clearing times using different exciters

t_{cr} (sec)	Exciter[a]
0.1923	#5
0.179	#1
0.160	#3
0.153	#4

[a]

Exciter	K	E_{FDmax}	τ_E (sec)
#1	145	8.85	0.05
#3	100	5.0	0.05
#4	45	4.0	0.10
#5	classical model		

These results are in agreement with the conclusions of reference [1, Chapter 8].

CHAPTER VII. CONCLUSION AND SUGGESTIONS FOR FUTURE WORK

This dissertation used the transient energy function technique, previously limited to classical power system models, to incorporate the effect of the exciter in first swing transient stability studies. A detailed representation of the generator along with excitation system has been used in direct methods to assess the transient stability of power systems of practical size with reasonable degree of success.

This success depended on the following:

1. The inertial nature of the first swing transient, i.e., the first swing transient is dominated by the inertial effects. As a result, the concepts of UEP and mode of disturbance developed for the classical model is valid. Detailed analysis of the components of the transient energy along the solution trajectory indicate that the critical trajectory passes "near" a UEP defined in the space of angular positions and internal generator voltages. In other words, the potential energy at the UEP determines the critical energy of the system.

2. A simple energy function using the two-axis model for the generator was obtained by assuming an average, but constant, value of E'_q and E'_d.

3. From the results presented in Chapters V and VI, the following conclusions are drawn:

   A. When the system configuration is such that the exciter does not change the mode of disturbance and/or the UEP corresponding to the given mode of disturbance can be determined.

      i. The assumption of constant E'_q and E'_d based on the average values between the disturbance clearing instant and the UEP reasonably accounts for the effect of the flux variations on the transient energy in the first swing.

ii. The resulting energy function is simple and easy to compute.

iii. Good transient stability assessment was obtained using this method for a) different kinds of simple faults, b) power transfer limits, and c) for generation shedding studies.

B. When the system configuration is such that the relevant UEP cannot be determined, the results are not satisfactory.

Suggestions for Future Work

The experience gained during this research project suggests the following subjects of investigation in order to enhance the applicability of the results presented in this dissertation.

1. Further investigation of the concept of the UEP defined in the extended space of angles and internal voltages, particularly when the exciter voltage reaches the limit. The issue to be clarified is that whether the condition

   $\frac{d}{dt} E_{FD} = 0$, assumed at the peak of the critical trajectory,

   is realistic.

2. Examination of the situations in which the system exhibits a complex mode of disturbance. Since the presence of modern exciters allows greater generator angle swing, the question arises as to whether the presence of the exciter complicates the search for the correct solution.

3. A more robust minimization algorithm for the UEP solution is needed. The Newton-Raphson technique used in this research project does not guarantee convergence. Usually, the second derivative information is needed in order to guarantee a "downhill" direction of search at each iterate. Is it possible to obtain the second derivative information effectively and computationally efficiently?

REFERENCES

1. Anderson, P. M., and A. A. Fouad. Power System Control and Stability. Ames: Iowa State University Press, 1977.

2. Brown, P. G., F. P. de Mello, E. H. Lenfest, and R. J. Mills. "Effects of Excitation, Turbine Energy Control and Transmission on Transient Stability." IEEE Trans. PAS-89, No. 6 (1970): 1247-1252.

3. de Mello, F. P., and C. Concordia. "Concepts of Synchronous Machine Stability as Affected by Excitation Control." IEEE Trans. PAS-88 (1969): 316-329.

4. IEEE Committee Report. "Proposed excitation system definitions for synchronous machines." IEEE Trans. PAS-88 (1969): 1248-1258.

5. Crary, S. B., "Long-Distance Power Transmission." AIEE Trans. 69 (1950): 834-844.

6. Concordia, C., and P. G. Brown. "Effects of Trends in Large Steam Turbine Driven Generator Parameters on Power System Stability." IEEE Trans. PAS-90 (1971): 2211-2218.

7. Concordia, C. "Maintaining Stability Following System Disturbances." Proceedings of the 1969 Minnesota Power Systems Conference, October 21-22, 1969, University of Minnesota, Minneapolis, Minnesota, 1969.

8. Modern Concepts of Power System Dynamics. IEEE tutorial course. IEEE Power Group Course Text 70 M 62-PWR, 1970.

9. Pai, M. A. Power System Stability. New York: North Holland Publishing Co., 1981.

10. Criteria of Stability of Electric Power Systems. A report. Union Institute of Scientific and Technological Information and the Academy of Sciences of the U.S.S.R. Electric Technology and Electric Power Series, Moscow, 1971.

11. Magnusson, P. C. "Transient Energy, Method of Calculating Stability." AIEE Trans. PAS-66 (1947): 747-755.

12. Aylett, P. D. "The Energy Integral Criterion of Transient Stability Limits of Power Systems." Proc. IEEE 105[C] (1958): 527-536.

13. Gless, G. E. "Direct Method of Lyapunov Applied to Transient Power System Stability." IEEE Trans. PAS-85 (February 1966): 158-168.

14. El-Abiad, A. H., and K. Nagappan. "Transient Stability Regions of Multimachine Power Systems." IEEE Trans. PAS-85 (February 1966): 158-168.

15. Fouad, A. A. "Stability Theory - Criteria for Transient Stability." Proc. Conference on Systems Engineering for Power: Status and Prospects, Henniker, NH, 1975.

16. Ribbens-Pavella, M. "Transient Stability of Multimachine Power Systems by Lyapunov's Direct Method." Proc. of Seminar on Stability of Large Scale Power Systems at the University of Liege, Liege, Belgium, 1972.

17. Athay, T., R. Podmore, and S. Virmani. "A Practical Method for Direct Analysis of Transient Stability." IEEE Trans. PAS-98 (1979): 573-584.

18. Athay, T., V. R. Sherket, R. Podmore, S. Virmani, and C. Puech. "Transient Energy Analysis." Proc. Conference on Systems Engineering for Power: Emergency Operating State Control, Davos, Switz., 1979.

19. Fouad, A. A., and S. E. Stanton. "Transient Stability Analysis of a Multi-Machine Power System. Part I: Investigation of System Trajectory; and Part II: Critical Transient Energy." IEEE Trans. PAS-100 (August 1981): 3408-3424.

20. Fouad, A. A., S. E. Stanton, K. R. C. Mamandur, and K. C. Kruempel. "Contingency Analysis Using the Transient Energy Margin Technique." Paper 815M397-9. IEEE PES Summer Meeting, Portland, OR, 1981.

21. Fouad, A. A., K. C. Kruempel, K. R. C. Mamandur, M. A. Pai, S. E. Stanton, and V. Vittal. "Transient Stability Margin as a Tool for Dynamic Security Assessment." Electrical Power Research Institute Report EL-1755, March 1981.

22. Vittal, V. "Power System Transient Stability Using the Critical Energy of Individual Machines." Ph.D. Dissertation. Iowa State University, Ames, Iowa, 1982.

23. Michel, A. N., A. A. Fouad, and V. Vittal. "Power System Transient Stability Using Individual Machine Energy Functions." IEEE Transactions on Circuits and Systems 30, No. 5 (1983): 266-276.

24. Fouad, A. A., V. Vittal, and T. Oh. "Critical Energy for Transient Stability Assessment of a Multimachine Power System." IEEE Trans. PAS-103 (1984): 2199-2206.

25. Siddiqee, M. W. "Transient Stability of an A.C. Generator by Lyapunov's Direct Method." Int. J. Control 8, No. 2 (1968): 131-144.

26. Pai, M. A., and Vishwanatha, Rai. "Lyapunov-Popov Stability Analysis of Synchronous Machine with Flux Decay and Voltage Regulator." Int. J. Control 19, No. 4 (1974): 817-829.

27. Sasaki, H. "An Appropriate Incorporation of Field Flux Decay into Transient Stability Analysis of Multimachine Power Systems by the Second Method of Lyapunov." IEEE Trans. Power Apparatus and Systems PAS-98, No. 2 (1979): 473-483.

28. Kakimoto, N., Y. Oshawa, and M. Hayashi. "Transient Stability Anslysis of Multimachine Power Systems with Field Flux Decays via Lyapunov's Direct Method." IEEE Trans. PAS-99, No. 5 (1980): 1819-1827.

29. Tsolas, N., A. Arapostatis, and P. Varaiya. "A Structure Preserving Energy Function for Power System Transient Stability Analysis." Memorandum M84/1. Electronics Research Laboratory, University of California, Berkeley, CA, January 3, 1984.

30. Bergen, A. R., and D. J. Hill. "A Structure Preserving Model for Power System Stability Analysis." IEEE Trans. PAS-100 (January 1981): 25-35.

31. IEEE Committee Report. "Excitation System Models for Power System Stability Studies." Prepared by the IEEE Working Group on Computer Modeling of Excitation Systems (F80 258-4). IEEE Trans. PAS 100 (February 81): 494-509.

32. EPRI Transient-Midterm Stability Program User Manual. EPRI EL-597 Project 745 User Manual. EPRI, Palo Alto, CA, 1979.

33. Kimbark, E. W. Power System Stabillity. Vol. I. New York: John Wiley & Sons, Inc., 1948. (Vol. I), 1950 (Vol. II), 1956 (Vol. (III).

34. Goldstein, H. Classical Mechanics. Cambridge, Mass.: Addison-Wesley Press, Inc., 1950.

35. Fouad, A. A., A. Ghafurian, K. Nodehi, and Y. Mansour. "Calculation of Generation-Shedding Requirements of the B.C. Hydro System Using Transient Energy Functions." IEEE Transactions on Power Systems, PWRS-1, No. 2 (May 1986): 17-24.

36. Fouad, A. A., A. Ghafurian, and K. Nodehi. "Analysis of Generation-Shedding on the B.C. Hydro System Using Transient Energy Functions." Final report submitted to B.C. Hydro. Iowa State University College of Engineering Report no. ISU-ERI-Ames-84508, September 1984.

ACKNOWLEDGMENTS

I would like to extend my deepest appreciation to my major professor and mentor Dr. A. A. Fouad. His rigorous involvement and technical guidance as well as his fatherly help and advice have made this research endeavor possible.

Special thanks are extended to Dr. Vijay Vittal whose continuous and active involvement as a member of my committee has been invaluable to this research endeavor.

I am also greatly thankful to the members of my committee: Dr. K. C. Kruempel whose help has always guided me through obstacles and problems, Dr. R. G. Brown, and Dr. R. J. Lambert.

I would like to thank Dr. H. R. Pota for his helpful involvement and suggestions.

I am indebted to the Electric Power Research Institute of Palo Alto, CA, and the Engineering Research Institute of Iowa State University for their financial support.

I also wish to thank Maggie Wheelock for typing this dissertation.

Finally, I would like to thank my family for their invaluable help and understanding. I am greatful to my parents for their great support and love despite hardships, and my wife for her understanding, kindness, and mental support.

I would like to dedicate this dissertation to my brother Shahriar whose brilliant mind and kind heart have always been my inspiration.

APPENDIX A. ENERGY FUNCTION DERIVATION

Terminal Voltage Formation

Let $\bar{V}_i = V_i \angle \beta_i$ be the terminal voltage of the generator i represented by the two-axis model. The accelerating power is given by:

$$\tilde{P}_{ai} = P_{Mi} - G_{ii}V_i^2 - \sum_{\substack{j=1 \\ j\neq i}}^{n} V_iV_j[G_{ij}\cos\beta_{ij} + B_{ij}\sin\beta_{ij}] - \frac{M_i}{M_T}P_{COI} \tag{A.1}$$

In equation (A.1), if i or j belong to the class of generators represented by the classical model, V and β must be replaced by E and θ, respectively. Neglecting the $(M_i/M_T)P_{COI}$ terms, the change in the potential energy can be obtained from:

$$V_{PE} = -\int_{\theta_i^{cl}}^{\theta_i^u} \sum_{i=1}^{n} \tilde{P}_{ai}\, d\theta_i$$

$$= -\sum_{i=1}^{n} P_{Mi}(\theta_i^u - \theta_i^{cl}) + \sum_{i=1}^{n}\int_{\theta_i^{cl}}^{\theta_i^u} G_{ij}V_i^2\, d\theta_i$$

$$+ \sum_{i=1}^{n-1}\sum_{j=i+1}^{n}\int_{\theta_{ij}^{cl}}^{\theta_{ij}^u} B_{ij}V_iV_j\sin\beta_{ij}\, d\theta_{ij}$$

$$+ \int_{\theta_i^{cl}+\theta_j^{cl}}^{\theta_i^u+\theta_j^u} G_{ij}V_iV_j\cos\beta_{ij}\, d(\theta_i + \theta_j) \tag{A.2}$$

$$\text{Let} \qquad \left.\begin{aligned} I_{Pei} &= \int V_i^2 \, d\theta_i \\ I_{sij} &= \int V_i V_j \sin \beta_{ij} \, d\theta_{ij} \\ I_{cij} &= \int V_i V_j \cos \beta_{ij} \, d(\theta_i + \theta_j) \end{aligned}\right\} \qquad (A.3)$$

We assume a linear dependence of V_i on θ_i, i.e.,

$$V_i = m_i \theta_i + c_i \ , \quad \beta_i = a_i \theta_i + k_i \qquad (A.4)$$

where i belongs to the set of generators represented by the two-axis model. In equation (A.4), the constants m and c are determined from the conditions at the instant of clearing the disturbance, and at the UEP.

Substituting (A.4) into (A.3) results in some path-dependent integrals. Similar to the derivation of the energy function for the classical model representation, a linear relation between θ_i and θ_j must be assumed. This assumption does not affect the path-independent integrals. Thus, the integrals are evaluated along the path $\theta_j = \lambda_{ij} \theta_i + \Gamma_{ij}$. By simple algebraic manipulations of (A.4) and the above linear path, it can be shown that

$$\left.\begin{aligned} \beta_{ij} &= g_{ij} \theta_{ij} + h_{ij} \\ \beta_{ij} &= r_{ij} (\theta_i + \theta_j) + s_{ij} \end{aligned}\right\} \qquad (A.5)$$

where

$$g_{ij} = \frac{a_i - a_j\lambda_{ij}}{1 - \lambda_{ij}}, \quad h_{ij} = \left(\frac{a_i - a_j}{1 - \lambda_{ij}}\right)\Gamma_{ij} + (k_i - k_j)$$

$$r_{ij} = \frac{a_i - a_j\lambda_{ij}}{1 + \lambda_{ij}}, \quad S_{ij} = -\left(\frac{a_i + a_j}{1 + \lambda_{ij}}\right)\Gamma_{ij} + (k_i - k_j)$$

The values of a, k, λ, and Γ are determined from the conditions at clearings and UEP.

Therefore, the integrals I_{Sij} and I_{Cij} of (A.3) can be written in the form:

$$\left.\begin{aligned} I_{Sij} &= (m_i m_j)I_{S1} + (m_i C_j)I_{S2} + (m_j C_i)I_{S3} + (C_i C_j)I_{S4} \\ I_{Cij} &= (m_i m_j)I_{C1} + (m_i C_j)I_{C2} + (m_j C_i)I_{C3} + (C_i C_j)I_{C4} \end{aligned}\right\} \quad (A.6)$$

where

$$I_{S1} = \int \theta_i\theta_j \sin\beta_{ij}\, d\theta_{ij}$$

$$I_{S2} = \int \theta_i \sin\beta_{ij}\, d\theta_{ij}$$

$$I_{S3} = \int \theta_j \sin\beta_{ij}\, d\theta_{ij}$$

$$I_{S4} = \int \sin\beta_{ij}\, d\theta_{ij}$$

$$I_{C1} = \int \theta_i\theta_j \cos\beta_{ij}\, d\theta_{ij}$$

$$I_{C2} = \int \theta_i \cos\beta_{ij}\, d\theta_{ij}$$

$$I_{C3} = \int \theta_j \cos \beta_{ij} \, d\theta_{ij}$$

$$I_{C4} = \int \cos\beta_{ij} \, d\theta_{ij}$$

By substituting (A.5) into (A.6), the integrals can be evaluated.

$$I_{S1} = \frac{\lambda_{ij}}{(1 - \lambda_{ij})^2} \left[- \frac{1}{g_{ij}} \theta_{ij}^2 \cos \beta_{ij} + \frac{2}{g_{ij}^2} \theta_{ij} \sin\beta_{ij} + \frac{2}{g_{ij}^3} \cos\beta_{ij} \right]$$

$$+ \frac{(1 + \lambda_{ij})\Gamma_{ij}}{(1 - \lambda_{ij})^2} \left[\frac{1}{g_{ij}^2} \sin \beta_{ij} - \frac{1}{g_{ij}} \theta_{ij} \cos \beta_{ij} \right]$$

$$- \frac{\Gamma_{ij}^2}{(1 - \lambda_{ij})^2} \left[\frac{1}{g_{ij}} \cos \beta_{ij} \right] \qquad \text{(A.7a)}$$

$$I_{S2} = \frac{1}{1 - \lambda_{ij}} \left[\frac{1}{g_{ij}^2} \sin \beta_{ij} - \frac{1}{g_{ij}} \theta_{ij} \cos \beta_{ij} \right]$$

$$- \frac{\Gamma_{ij}}{1 - \lambda_{ij}} \left[\frac{1}{g_{ij}} \cos \beta_{ij} \right] \qquad \text{(A.7b)}$$

$$I_{S3} = \frac{\lambda_{ij}}{1 - \lambda_{ij}} \left[\frac{1}{g_{ij}^2} \sin \beta_{ij} - \frac{1}{g_{ij}} \theta_{ij} \cos \beta_{ij} \right]$$

$$- \frac{\Gamma_{ij}}{1 - \lambda_{ij}} \left[\frac{1}{g_{ij}} \cos \beta_{ij} \right] \qquad \text{(A.7c)}$$

$$I_{S4} = -\frac{1}{g_{ij}} \cos \beta_{ij} \tag{A.7d}$$

$$I_{C1} = \frac{1}{(1 + \lambda_{ij})^2} \left[\frac{1}{r_{ij}} (\theta_i + \theta_j)^2 \sin \beta_{ij} \right.$$

$$\left. + \frac{2}{r_{ij}^2} (\theta_i + \theta_j) \cos \beta_{ij} - \frac{2}{r_{ij}^3} \sin \beta_{ij} \right]$$

$$+ \frac{\Gamma_{ij}(1 - \lambda_{ij})}{1 + \lambda_{ij}} \left[\frac{1}{r_{ij}^2} \cos \beta_{ij} + \frac{1}{r_{ij}} (\theta_i + \theta_j) \sin \beta_{ij} \right]$$

$$- \frac{\Gamma_{ij}^2}{(1 + \lambda_{ij})^2} \left[\frac{1}{r_{ij}} \sin \beta_{ij} \right] \tag{A.7e}$$

$$I_{C2} = \frac{1}{1 + \lambda_{ij}} \left[\frac{1}{r_{ij}^2} \cos \beta_{ij} + \frac{1}{r_{ij}} (\theta_i + \theta_j) \sin \beta_{ij} \right]$$

$$- \frac{\Gamma_{ij}}{1 + \lambda_{ij}} \left[\frac{1}{r_{ij}} \sin \beta_{ij} \right] \tag{A.7f}$$

$$I_{C3} = \frac{\lambda_{ij}}{1 + \lambda_{ij}} \left[\frac{1}{r_{ij}^2} \cos \beta_{ij} + \frac{1}{r_{ij}} (\theta_i + \theta_j) \sin \beta_{ij} \right]$$

$$+ \frac{\Gamma_{ij}}{1 + \lambda_{ij}} \left[\frac{1}{r_{ij}} \sin \beta_{ij} \right] \tag{A.7g}$$

$$I_{C4} = \frac{1}{r_{ij}} \sin \beta_{ij} \tag{A.7h}$$

Note that the integrals of (A.7) must be evaluated between the clearing instant and the UEP.

The change in potential energy, ΔV_{PE}, is given by:

$$\Delta V_{PE} = -\sum_{i=1}^{n} P_{Mi}(\theta_i^u - \theta_i^{cl}) + \sum_{i=1}^{n} G_{ij}\left[\left(\frac{1}{3} m_i^2\right)\theta_i^3 + (m_i C_i)\theta_i^2 + (C_i^2)\theta_i\right]\Bigg|_{\theta_i^{cl}}^{\theta_i^u}$$

$$+ \sum_{i=1}^{n-1}\sum_{j=i+1}^{n}\left[B_{ij} I_{Sij}\Big|_{\theta_{ij}^{cl}}^{\theta_{ij}^u} + G_{ij} I_{Cij}\Big|_{\theta_{ij}^{cl}}^{\theta_{ij}^u}\right] \qquad (A.8)$$

The kinetic energy expression is similar to that of the classical model representation and it is given by:

$$V_{KE} = \sum_{i=1}^{n} \frac{1}{2} M_i \tilde{\omega}_i^2 \qquad (A.9)$$

The energy margin is obtained from:

$$V\Big|_{cl}^{UEP} \triangleq \Delta V = \Delta V_{PE} - V_{KE} \qquad (A.10)$$

E' Formulation (linear E')

Let $E_i' \angle \gamma_i$ be the voltage behind the transient reactance of the generators represented by the two-axis model (see Figures 4.4 and 4.5). The accelerating power in the center of inertia frame is given by:

$$\tilde{P}_{ai} = P_{Mi} - \left[G_{ii} E_i'^2 + \sum_{\substack{i=1 \\ j\neq i}}^{n} E_i' E_j' (B_{ij} \sin \gamma_{ij} + G_{ij} \cos \gamma_{ij})\right] - \frac{M_i}{M_T} P_{COI} \qquad (A.11)$$

In equation (A.11), if i or j belong to the class of generators represented by the classical model, E' and γ must be replaced by E and θ, respectively.

The change in the potential energy is obtained by integrating the accelerating powers with respect to angles θ as follows:

$$\Delta V_{PE} = \sum_{i=1}^{n} \int_{\theta_i^{cl}}^{\theta_i^u} (-\tilde{P}_{ai}) d\theta_i$$

$$= -\sum_{i=1}^{n} P_{Mi}(\theta_i^u - \theta_i^{cl}) + \sum_{i=1}^{n} G_{ii} \int_{\theta_i^{cl}}^{\theta_i^u} E_i'^2 \, d\theta_i$$

$$+ \sum_{i=1}^{n-1} \sum_{j=i+1}^{n} \left[B_{ij} \int_{\theta_{ij}^{cl}}^{\theta_{ij}^u} E_i' E_j' \sin \gamma_{ij} \, d\theta_{ij} \right.$$

$$\left. + G_{ij} \int_{\theta_i^{cl}+\theta_j^{cl}}^{\theta_i^u+\theta_i^u} E_i' E_j' \cos \gamma_{ij} \, d(\theta_i + \theta_j) \right] \qquad \text{(A.12)}$$

For the generators represented by the two-axis model, we assume the following:

$$E_i' = m_i \theta_i + C_i \qquad \text{(A.13)}$$

$$\gamma_i = \theta_i + \alpha_i^{cl} \qquad \text{(A.14)}$$

where the constants m and C are determined from the conditions at the

instant of clearing the disturbance and at the UEP. Thus, the integrals in (A.12) can be written in the form:

$$I_{Pi} = \int E_i'^2 \, d\theta_i$$

$$= \int [m_i^2\theta_i^2 + 2m_iC_i\theta_i + C_i^2]d\theta_i \qquad \text{(A.15)}$$

$$I_{Sij} = \int E_i'E_j' \sin \gamma_{ij} \, d\theta_i \qquad \text{(A.16)}$$

$$= \int [(m_im_j)\theta_i\theta_j + (m_iC_j)\theta_i + (m_jC_i)\theta_j + (C_iC_j)]\sin(\theta_{ij} + \alpha_{ij}^{cl})d\theta_{ij}$$

$$I_{Cij} = \int E_i'E_j' \cos \gamma_{ij} \, d(\theta_i + \theta_j)$$

$$= \int [(m_im_j)\theta_i\theta_j + (m_iC_j)\theta_i + (m_jC_i)\theta_j + (C_iC_j)] \qquad \text{(A.17)}$$

$$\times \cos(\theta_{ij} + \alpha_{ij}^{cl})d(\theta_i + \theta_j)$$

The integrals of (A.15) and (A.16) are evaluated along the path $\theta_j = \lambda_{ij}\theta_{ij} + \Gamma_{ij}$. Thus,

$$I_{Pi} = (\tfrac{1}{3} m_i^2)\theta_i^3 + (m_iC_i)\theta_i^2 + (C_i^2)\theta_i \qquad \text{(A.18)}$$

$$I_{Sij} = \frac{\lambda_{ij}}{(1 - \lambda_{ij})^2} \left[- \theta_{ij}^2 \cos(\theta_{ij} + \alpha_{ij}^{cl}) + 2\theta_{ij} \sin(\theta_{ij} + \alpha_{ij}^{cl}) \right.$$

$$\left. + 2 \cos(\theta_{ij} + \alpha_{ij}^{cl}) \right]$$

$$+\frac{1+\lambda_{ij}}{1-\lambda_{ij}}\left(1+\frac{\Gamma_{ij}}{1-\lambda_{ij}}\right)\left[\sin(\theta_{ij}+\theta_{ij}^{cl})-\theta_{ij}\cos(\theta_{ij}+\alpha_{ij}^{cl})\right]$$

$$-\left(1+\frac{\Gamma_{ij}}{1-\lambda_{ij}}\right)^{2}\cos(\theta_{ij}+\alpha_{ij}^{cl}) \qquad (A.19)$$

$$I_{Cij}=\frac{1}{(1+\lambda_{ij})^{2}}\left[b_{ij}(\theta_i+\theta_j)^{2}\sin(\theta_{ij}+\alpha_{ij}^{cl})\right.$$

$$\left.+2b_{ij}^{2}(\theta_i+\theta_j)\cos(\theta_{ij}+\alpha_{ij}^{cl})-2b_{ij}^{3}\sin(\theta_{ij}+\alpha_{ij}^{cl})\right]$$

$$+\left(1+\frac{1-\lambda_{ij}}{1+\lambda_{ij}}\Gamma_{ij}\right)\left[b_{ij}^{2}\cos(\theta_{ij}+\alpha_{ij}^{cl})+b_{ij}(\theta_i+\theta_j)\right.$$

$$\left.\times\sin(\theta_{ij}+\alpha_{ij}^{cl})\right]-\left(\frac{\Gamma_{ij}^{2}}{(1+\lambda_{ij})^{2}}-1\right)b_{ij}\sin(\theta_{ij}+\alpha_{ij}^{cl}) \qquad (A.20)$$

where $b_{ij}=\dfrac{1+\lambda_{ij}}{1-\lambda_{ij}}$

Therefore, the change in the potential energy is obtained from:

$$\Delta V_{PE}=-\sum_{i=1}^{n}P_{Mi}(\theta_i^{u}-\theta_i^{cl})+\sum_{i=1}^{n}G_{ii}I_{Pi}\Big|_{\theta_i^{cl}}^{\theta_i^{u}}$$

$$+\sum_{i=1}^{n-1}\sum_{j=i+1}^{n}\left[B_{ij}I_{Sij}\Big|_{\theta_{ij}^{cl}}^{\theta_{ij}^{u}}+G_{ij}I_{Cij}\Big|_{\theta_{ij}^{cl}}^{\theta_{ij}^{u}}\right] \qquad (A.21)$$

The kinetic energy and the energy margin are given in equations (A.9) and (A.10).

Constant E'_q and E'_d Formulation

For a generator represented by the two-axis model, the electrical power, assuming $x'_d = x'_q$, is given by

$$P_{ei} = E'_{di} I_{di} + E'_{qi} I_{qi} \tag{A.22}$$

The currents I_{di} and I_{qi} are computed from

$$I_{di} = \sum_{j=1}^{n} F_{B-G}(\theta_{ij}) E'_{qj} + F_{G+B}(\theta_{ij}) E'_{dj} \tag{A.23a}$$

$$I_{qi} = \sum_{j=1}^{n} F_{G+B}(\theta_{ij}) E'_{qj} - F_{B-G}(\theta_{ij}) E'_{dj} \tag{A.23b}$$

where

$$F_{G+B}(\theta_{ij}) = G_{ij} \cos \theta_{ij} + B_{ij} \sin \theta_{ij} \tag{A.24a}$$

$$F_{B-G}(\theta_{ij}) = B_{ij} \cos \theta_{ij} - G_{ij} \sin \theta_{ij} \tag{A.24b}$$

In equations (A.22) and (A.23), E'_q and E'_d must be replaced with E and 0 when i or j belong to the set of generators represented by the classical model.

Substituting (A.23) into (A.22) and rearranging terms results in

$$P_{ei} = \sum_{j=1}^{n} \left[\alpha_{ij} F_{G+B}(\theta_{ij}) + \beta_{ij} F_{B-G}(\theta_{ij}) \right] \tag{A.25}$$

where

$$\alpha_{ij} = E'_{di}E'_{dj} + E'_{qi}E'_{qj} \tag{A.26a}$$

$$\beta_{ij} = E'_{di}E'_{qj} - E'_{qi}E'_{dj} \tag{A.26b}$$

By substituting (A.24) into (A.25), the electrical power of generator i can be expressed in the following form

$$P_{ei} = \alpha_{ii}G_{ii} + \sum_{\substack{j=1 \\ j\neq i}}^{n} \Big[B_{ij}(\alpha_{ij} \sin \theta_{ij} + \beta_{ij} \cos \theta_{ij}) + G_{ij}(\alpha_{ij} \cos \theta_{ij} - \beta_{ij} \sin \theta_{ij}) \Big] \tag{A.27}$$

Thus,

$$\tilde{P}_{ai} = P_{Mi} - P_{ei} - \frac{M_i}{M_T} P_{COI} \tag{A.28}$$

The total energy is obtained by multiplying $M_i\dot{\tilde{\omega}}_i - P_{ai}$ by $\tilde{\omega}_i$, summing over i = 1, 2, ..., n, and integrating with respect to time. Thus,

$$V = \sum_{i=1}^{n} \int M_i\dot{\tilde{\omega}}_i \, \tilde{\omega} dt + \sum_{i=1}^{n} \int (-\tilde{P}_{ai}) d\theta_i$$

$$= \sum_{i=1}^{n} \frac{1}{2} M_i\tilde{\omega}_i^2 + \sum_{i=1}^{n} \int (-\tilde{P}_{ai}) d\theta_i \tag{A.29}$$

where the first term is the kinetic energy, and the second term is the

potential energy of the system. The expression for the change in potential energy is given by

$$\Delta V_{PE} = \sum_{i=1}^{n} \int_{\theta_i^{cl}}^{\theta_i^u} (-\tilde{P}_{ai}) d\theta_i$$

$$= \sum_{i=1}^{n} - P_{Mi}(\theta_i^u - \theta_i^{cl}) + \sum_{i=1}^{n} \int_{\theta_i^{cl}}^{\theta_i^u} P_{ei} d\theta_i \qquad (A.30)$$

Substituting for P_{ei} from (A.27) into equation (A.30) and using $\alpha_{ij} = \alpha_{ji}$ and $\beta_{ij} = -\beta_{ji}$, equation (A.30) can be rearranged as follows

$$\Delta V_{PE} = \sum_{i=1}^{n} - P_{Mi}\, d\theta_i + \sum_{i=1}^{n} \int_{\theta_i^{cl}}^{\theta_i^u} G_{ii}\alpha_{ii} d\theta_i$$

$$+ \sum_{i=1}^{n-1} \sum_{j=i+1}^{n} B_{ij} \left[\int_{\theta_{ij}^{cl}}^{\theta_{ij}^u} \alpha_{ij} \sin \theta_{ij}\, d\theta_i + \int_{\theta_{ij}^{cl}}^{\theta_{ij}^u} \beta_{ij} \cos \theta_{ij}\, d\theta_{ij} \right]$$

$$+ \sum_{i=1}^{n-1} \sum_{j=i+1}^{n} G_{ij} \left[\int_{\theta_i^{cl}+\theta_j^{cl}}^{\theta_i^u+\theta_j^u} \alpha_{ij} \cos \theta_{ij}\, d(\theta_i + \theta_j) \right.$$

$$\left. - \int_{\theta_i^{cl}+\theta_j^{cl}}^{\theta_i^u+\theta_j^u} \beta_{ij} \sin \theta_{ij}\, d(\theta_i + \theta_j) \right] \qquad (A.31)$$

Assume that E_q' and E_d' are held constant at their average value, i.e., $E_q' = \frac{1}{2}(E_q'^u + E_q'^{cl})$, $E_d' = \frac{1}{2}(E_d'^u + E_d'^{cl})$. Thus, the values of α and β

are fixed in (A.31). The last two integrals of (A.31) are path-dependent integrals. Similar to the derivation of the energy function for the classical model a linear path, i.e., $\theta_j = (\text{constant})\theta_i$ is assumed and integration is done along this path. The value of the constant is determined from the conditions at the clearing of the disturbance and the UEP. Thus, the change in the potential energy is given by:

$$\Delta V_{PE} = \sum_{i=1}^{n} - P_{Mi}(\theta_i^u - \theta_i^{cl}) + \sum_{i=1}^{n} \alpha_{ii} G_{ii} (\theta_i^u - \theta_i^{cl})$$

$$+ \sum_{i=1}^{n-1} \sum_{j=i+1}^{n} B_{ij} \left[\alpha_{ij} (-\cos \theta_{ij}^u + \cos \theta_{ij}^{cl}) \right.$$

$$\left. + \beta_{ij} (\sin \theta_{ij}^u - \sin \theta_{ij}^{cl}) \right]$$

$$+ \sum_{i=1}^{n-1} \sum_{j=i+1}^{n} G_{ij} \frac{\theta_i^u + \theta_j^u - \theta_i^{cl} - \theta_j^{cl}}{\theta_{ij}^u - \theta_{ij}^{cl}}$$

$$\times \left[\alpha_{ij} (\sin \theta_{ij}^u - \sin \theta_{ij}^{cl}) + \beta_{ij} (\cos \theta_{ij}^u - \cos \theta_{ij}^{cl}) \right] \tag{A.32}$$